frontiers

The Developing Human Connectome Project Neonatal Data Release

A David Edwards[1, 2*], Daniel Rueckert[3, 4], Stephen M. Smith[5], Sami Abo Seada[6], Amir Alansary[4], Jenie Almalbis[1], Joanna M. Allsop[1], Tomoki Arichi[2, 1], Jesper Andersson[5], Sophie Arulkumaran[1], Matteo Bastiani[5, 7], Dafnis Batalle[1, 8], Luke Baxter[5], Jelena Bozek[5], Eleanor Braithwaite[9], Jacqueline Brandon[1], Olivia Carney[1], Andrew Chew[1], Daan Christiaens[1, 10], Raymond Chung[11], Kathleen Colford[1], Lucilio Cordero-Grande[1, 12], Serena J. Counsell[1], Harriet Cullen[1, 13], John Cupitt[14], Charles Curtis[11], Alice Davison[1], Maria Deprez[1, 6], Louise Dillon[1], Konstantina Dimitrakapoulou[1, 15], Rali Dimitrova[1, 8], Eugene Duff[5, 16], Shona Falconer[1], Revzan Farahibozorgwe[5], Sean Fitzgibbon[5], Jianliang Gao[4], Andreia S. Gaspar[17], Nicholas Harper[1], Samuel J. Harrison[5], Emer J. Hughes[1], Jana Hutter[1, 6], Mark Jenkinson[5], Saad Jbabdi[5], Emily Jones[9], Vyacheslav Karolis[1, 5], Vanessa Kyriakopoulou[1], Gregor Lenz[4], Antonis Makropoulos[1, 4], Shaihan Malik[1, 6], Filippo Mortari[4], Chiara Nosarti[18, 1], Rita G. Nunes[17, 1], Camilla O'Keefe[1], Jonathan O'Muircheartaigh[1, 2, 8], Hamel Patel[11], Jonathan Passerat-Palmbach[4], Maximillian Pietsch[1, 8], Anthony N. Price[1, 6], Emma Robinson[1, 6], Mary A. Rutherford[1], Andreas Schuh[4], Stamatios Sotiropoulos[7, 5], Johannes K. Steinweg[1], Rui P. Teixeira[1, 6], Tencho Tenev[4], J-Donald Tournier[1, 6], Nora Tusor[1], Alena Uus[1, 19], Katy Vecchiato[1], Logan Z. Williams[1, 6], Robert Wright[4], Julia Wurie[1], Joseph V. Hajnal[1, 6]

[1]Centre for the Developing Brain, King's College London, United Kingdom, [2]MRC Centre for Neurodevelopmental Disorders, King's College London, United Kingdom, [3]Technical University of Munich, Germany, [4]Biomedical Image Analysis Group, Department of Computing, Imperial College London, United Kingdom, [5]Wellcome Centre For Integrative Neuroimaging, Nuffield Department of Clinical Neurosciences, Medical Sciences Division, University of Oxford, United Kingdom, [6]Department of Biomedical Engineering, School of Biomedical Engineering & Imaging Sciences, Faculty of Life Sciences & Medicine, King's College London, United Kingdom, [7]Sir Peter Mansfield Imaging Centre, University of Nottingham, United Kingdom, [8]Department of Forensic and Neurodevelopmental Sciences, Institute of Psychiatry, Psychology & Neuroscience, King's College London, United Kingdom, [9]Centre for Brain and Cognitive Development, School of Science, Birkbeck University of London, United Kingdom, [10]Department of Electrical Engineering, KU Leuven, Belgium, [11]NIHR Maudsley Biomedical Research Centre (BRC), United Kingdom, [12]Escuela Técnica Superior de Ingeniería Informática, Universidad Politécnica de Madrid, Spain, [13]Department of Medical and Molecular Genetics, School of Basic & Medical Biosciences, Faculty of Life Sciences & Medicine, King's College London, United Kingdom, [14]Department of Computing, Faculty of Engineering, Imperial College London, United Kingdom, [15]Translational Bioinformatics Platform, NIHR Biomedical Research Centre, Guy's and St Thomas' NHS Foundation Trust and King's College London, United Kingdom, [16]Department of Brain Sciences, Faculty of Medicine, Imperial College London, United Kingdom, [17]Instituto Superior Técnico, Universidade de Lisboa, Portugal, [18]Department of Child and Adolescent Psychiatry, Institute of Psychiatry, Psychology and Neuroscience, King's College London, United Kingdom, [19]School of Biomedical Engineering & Imaging Sciences, Faculty of Life Sciences & Medicine, King's College London, United Kingdom

Submitted to Journal:
Frontiers in Neuroscience

Specialty Section:
Brain Imaging Methods

Article type:
Original Research Article

Manuscript ID:
886772

Received on:
28 Feb 2022

Conflict of interest statement

The authors declare that the research was conducted in the absence of any commercial or financial relationships that could be construed as a potential conflict of interest

Author contribution statement

Attained funding: ADE, DR, SMS, JVH. Developed acquisition methods: SAS, LCG, ASG, EJH, JH, SM, RGN, ANP, RT, JDT, JVH. Collected data: JA, JA, TA, SA, JB, AC, KC, RC, AD, LD, SF, NH, EJH, CO, HP, JS, NT, KV, JW. Developed analysis methods: DR, SMS, AA, JA, TA, MB, LB, JB, DC, JC, SJC, MD, ED, SF, SPF, JG, SJH, MJ, SJ, VK, GL, AM, FM, JOM, JPP, MP. ECR, AS, SNS, TT, JDT, AU, RW, JVH. Analysed data: ADE, SMS, TA, SA, DB, LB, EB, OC, DC, RD, ED, EJ, VK, CN, JOM, MP, MAR, LZJW. Prepared manuscript: ADE, DR, TA, DC, HC, KD, SF, NH, VK, MP, ANP, JVH. All authors have reviewed the manuscript.

Keywords

Developing human connectome project, DHCP, Brain Development, MRI, neonatal, connectome, perinatal

Abstract

Word count: 190

The Developing Human Connectome Project has created a large open science resource which provides researchers with data for investigating typical and atypical brain development across the perinatal period. It has collected 1228 multimodal magnetic resonance images of fetal and/or neonatal brain from 1173 participants, together with collateral demographic, clinical, family, neurocognitive and genomic data. All subjects were studied in utero and/or soon after birth on a single MRI scanner using specially developed scanning sequences which included novel motion-tolerant imaging methods. Imaging data are complemented by rich demographic, clinical, neurodevelopmental, clinical, and genomic information. The project is now releasing a large set of neonatal data; fetal data will be described and released separately. This release includes scans from 783 infants of whom: 583 were healthy infants born at term; as well as preterm infants; and infants at high risk of atypical neurocognitive development. Many infants were imaged more than once to provide longitudinal data, and the total number of datasets being released is 887. We now describe the dHCP image acquisition and processing protocols, summarize the available imaging and collateral data, and provide information on how the data can be accessed.

Contribution to the field

The Developing Human Connectome Project has created a large open science resource which provides researchers with data for investigating typical and atypical brain development across the perinatal period. It has collected 1228 multimodal magnetic resonance images of fetal and/or neonatal brain from 1173 participants, together with collateral demographic, clinical, family, neurocognitive and genomic data. All subjects were studied in utero and/or soon after birth on a single MRI scanner using specially developed scanning sequences which included novel motion-tolerant imaging methods. Imaging data are complemented by rich demographic, clinical, neurodevelopmental, clinical, and genomic information. The project is now releasing a large set of neonatal data; fetal data will be described and released separately. This release includes scans from 783 infants of whom: 583 were healthy infants born at term; as well as preterm infants; and infants at high risk of atypical neurocognitive development. Many infants were imaged more than once to provide longitudinal data, and the total number of datasets being released is 887. We now describe the dHCP image acquisition and processing protocols, summarize the available imaging and collateral data, and provide information on how the data can be accessed.

Funding statement

The Developing Human Connectome Project was funded by the European Research Council under the European Union Seventh Framework Programme (FP/20072013)/ERC Grant Agreement no. 319456. The work was supported by: the NIHR Biomedical Research Centres at Guys and St Thomas NHS Trust and the South London and Maudsley NHS Trust; the ESPRC/Wellcome Centre for Medical Engineering; and the MRC Centre for Neurodevelopmental Disorders.

TA is supported by a MRC Clinician Scientist Fellowship [MR/P008712/1] and MRC translation support award [MR/V036874/1]. JOM is supported by a Sir Henry Dale Fellowship jointly funded by the Wellcome Trust and the Royal Society [Grant Number 206675/Z/17/Z].

Ethics statements

Studies involving animal subjects

Generated Statement: No animal studies are presented in this manuscript.

Studies involving human subjects

Generated Statement: The studies involving human participants were reviewed and approved by UK Health Research Authority (Research Ethics Committee reference number: 14/LO/1169) . Written informed consent to participate in this study was provided by the participants' legal guardian/next of kin.

Inclusion of identifiable human data

Generated Statement: No potentially identifiable human images or data is presented in this study.

Data availability statement

Generated Statement: The datasets presented in this study can be found in online repositories. The names of the repository/repositories and accession number(s) can be found below:
http://www.developingconnectome.org/data-release/third-data-release/, 1
https://nda.nih.gov/edit_collection.html?id=3955, 3955.

The Developing Human Connectome Project Neonatal Data Release

AD Edwards[1,2], D Rueckert[3,4], SM Smith[5], S Abo Seada[6], A Alansary[3], J Almalbis[1], J Allsop[1], J Andersson[5], T Arichi[1,2], S Arulkumaran[1], M Bastiani[5,7], D Batalle[1,8], L Baxter[5], J Bozek[5], Braithwaite E[9], J Brandon[1], O Carney[1], A Chew[1], D Christiaens[1,10], R Chung[11], K Colford[1], L Cordero-Grande[1,12], SJ Counsell[1], H Cullen[1,13], J Cupitt[3], C Curtis[11], A Davidson[1], M Deprez[1,6], L Dillon[1], K Dimitrakopoulou[1,14], R Dimitrova[1,8], E Duff[5], S Falconer[1], SR Farahibozorg[5], SP Fitzgibbon[5], J Gao[3], AS Gaspar[15] , N Harper[1], SJ Harrison[5], EJ Hughes[1], J Hutter[1,6], M Jenkinson[5], S Jbabdi[5], E Jones[9], V Karolis[1,5], V Kyriakopoulou[1], G Lenz[3], A Makropoulos[1,3], S Malik[1,6], L Mason[9], F Mortari[3], C Nosarti[1,16], RG Nunes[1,15], C O'Keeffe[1], J O'Muircheartaigh[1,2,8], H Patel[11], J Passerat-Palmbach[3], M Pietsch[1,8], AN Price[1,6], EC Robinson[1,6], MA Rutherford[1], A Schuh[3], SN Sotiropoulos[5,7], J Steinweg[1], R Teixeira[1,6], T Tenev[3], JD Tournier[1,6], N Tusor[1], A Uus[1,6], K Vecchiato[1], LZJ Williams[1], R Wright[3], J Wurie[1], JV Hajnal[1,6].

1. Centre for the Developing Brain, School of Biomedical Engineering and Imaging Sciences, King's College London, London UK.
2. MRC Centre for Neurodevelopmental Disorders, King's College London, UK.
3. Biomedical Image Analysis Group, Department of Computing, Imperial College London, UK.
4. Institute for AI and Informatics in Medicine, Klinikum rechts der Isar, Technical University of Munich, Munich, Germany.
5. Wellcome Centre for Integrative Neuroimaging, FMRIB, Nuffield Department of Clinical Neurosciences, University of Oxford, UK.
6. Biomedical Engineering Department, School of Biomedical Engineering & Imaging Sciences, King's College London, London, UK.
7. Sir Peter Mansfield Imaging Centre, Mental Health and Clinical Neurosciences, School of Medicine, University of Nottingham, UK
8. Department of Forensic and Neurodevelopmental Sciences, Institute of Psychiatry, Psychology & Neuroscience, King's College London, London SE5 8AF, UK.
9. Centre for Brain and Cognitive Development, Department of Psychological Sciences, Birkbeck, University of London, London, UK.
10. Department of Electrical Engineering, ESAT/PSI, KU Leuven, Leuven, Belgium
11. BioResource Centre, NIHR Biomedical Research Centre, South London and Maudsley NHS Trust
12. Biomedical Image Technologies, ETSI Telecomunicación, Universidad Politécnica de Madrid & CIBER-BBN, Madrid, Spain
13. Department of Medical and Molecular Genetics, School of Basic and Medical Biosciences, King's College London, London SE1 9RT
14. Translational Bioinformatics Platform, NIHR Biomedical Research Centre, Guy's and St Thomas' NHS Foundation Trust and King's College London, London, UK
15. Institute for Systems and Robotics (ISR-Lisboa)/LaRSyS, Department of Bioengineering, Instituto Superior Técnico, Universidade de Lisboa, Lisbon, Portugal
16. Department of Child and Adolescent Psychiatry, Institute of Psychiatry, Psychology and Neuroscience, King's College London, London, UK

*Corresponding author:
Professor A David Edwards, Centre for the Developing Brain, School of Biomedical Engineering and Imaging Sciences, King's College London, London, SE1 7EH, UK. Email: ad.edwards@kcl.ac.uk

KEYWORDS:
Developing Human Connectome Project, dHCP, Brain development, MRI, Neonatal, Newborn, Connectome, Perinatal.

Abstract

The Developing Human Connectome Project has created a large open science resource which provides researchers with data for investigating typical and atypical brain development across the perinatal period. It has collected 1228 multimodal magnetic resonance images of fetal and/or neonatal brain from 1173 participants, together with collateral demographic, clinical, family, neurocognitive and genomic data. All subjects were studied in utero and/or soon after birth on a single MRI scanner using specially developed scanning sequences which included novel motion-tolerant imaging methods. Imaging data are complemented by rich demographic, clinical, neurodevelopmental, clinical, and genomic information. The project is now releasing a large set of neonatal data; fetal data will be described and released separately. This release includes scans from 783 infants of whom: 583 were healthy infants born at term; as well as preterm infants; and infants at high risk of atypical neurocognitive development. Many infants were imaged more than once to provide longitudinal data, and the total number of datasets being released is 887. We now describe the dHCP image acquisition and processing protocols, summarize the available imaging and collateral data, and provide information on how the data can be accessed.

Introduction

Recent advances in MRI acquisition, image processing and analysis have it made it possible to gain a non-invasive yet detailed multimodal characterization of the human brain's macroscopic connections (Craddock et al., 2013). Novel connectivity maps encompass not only the structural connections relating to white matter tracts, but the functional connections revealed by coordinated grey-matter activations, and connectivity related to coordinated development revealed in structural covariance (Alexander-Bloch et al., 2013) and multimodal similarity networks (Seidlitz et al., 2018). The value of these approaches has been highlighted in recent years by the Human Connectome Project (HCP), which has fostered growing interest in the science of connectomics and become a critical resource for research into the mature human brain (Van Essen et al., 2013).

Human brain development accelerates rapidly in late pregnancy to reach maximum global growth rate before 6 months (Bethlehem et al., 2022). This rapid growth is accompanied by equally dramatic changes in the brain's associated architecture of structural and functional connectivity, and therefore understanding these processes in both the healthy and pathological brain can provide marked new insights into fundamental neural processes and the possible changes that underlie intractable neuropsychiatric conditions. However, characterization of this process has previously been limited by the challenges inherent in safely and robustly studying the brain during this vulnerable phase of life. The Developing Human Connectome Project (dHCP) is an open science study, funded by the European Research Council to obtain and disseminate Magnetic Resonance Imaging (MRI) data which map the brain's structural and functional development across the period from 20 weeks gestational age to full term. By coupling advances in imaging with bespoke solutions developed for the fetal and neonatal population, principally but not exclusively solving the problems of subject motion, the dHCP captures the development of brain anatomy and connectivity at a systems level. This enables exploration of maturational trajectories, structure and function relationships, the neural substrates for behaviour and cognition, and the influences of genetic and environmental factors. The dHCP includes both in utero imaging of fetal brain and postnatal imaging of preterm and term born infants, capturing typical and atypical brain development. It has created maps of the developing human brain and its connections as a resource for the neuroscience community and a platform for connectome research.

The dHCP dataset includes a large number of healthy, term-born infants which allow definition of typical development with previously unobtainable precision. It is increasingly appreciated that the perinatal period is crucial for lifelong brain health, and multiple lines of evidence show that early life

influences have a critical effect on brain circuitry in later childhood and adult life (Batalle et al., 2018). This has key implications for understanding the pathophysiology of neurodevelopmental conditions, such as autism (Hisle-Gorman et al., 2018) or the difficulties associated with preterm birth (Montagna and Nosarti, 2016). Understanding these effects has important clinical implications, and to support relevant investigations clinical and demographic data were collected and saliva samples obtained for genetic and epigenetic analysis, with participating families invited back at 18 months of age for a developmental assessment using standard tests and questionnaires, including eye-tracking studies.

A key priority for the project was that the data be made available to the research community, and preliminary data releases (www.developingconnectome.org) have been accessed and used by a number of research groups. We now describe the main neonatal data release, providing a summary of the participants, the MR imaging data acquisition and processing, the collateral data including sociodemographic and neuropsychological outcome data, and the genomic data. We also describe available data for each category and how to obtain it. Fetal data will be described and released separately.

Participants

Infants were recruited at St Thomas' Hospital, London and imaged at the Evelina Newborn Imaging Centre, Centre for the Developing Brain, King's College London, UK. The MR suite is sited within the neonatal intensive care unit which allows imaging of even the smallest and most vulnerable newborn infants, as well as having proximity to the maternity unit to support fetal scanning.

The images of 783 newborn infants are being released. Infants were recruited with specified inclusion and exclusion criteria (http://www.developingconnectome.org/study-inclusion-and-exclusion-criteria/) across a spread of gestational ages at birth (range: 23 to 43+1 weeks + days) and postmenstrual ages at the time of study (range: 26+5 to 45+1). The distributions of gestational age at birth and postmenstrual age at scan are shown in figure 1.

The study population includes 583 subjects were born at term equivalent age (37 to 44 weeks post-menstrual age) without any known pregnancy or neonatal problems and are regarded as healthy. All the anatomical images were reviewed by an expert perinatal neuroradiologist and radiologic scores included in the released data. Incidental findings noted in a proportion and a report on these has been published (Carney et al., 2021).

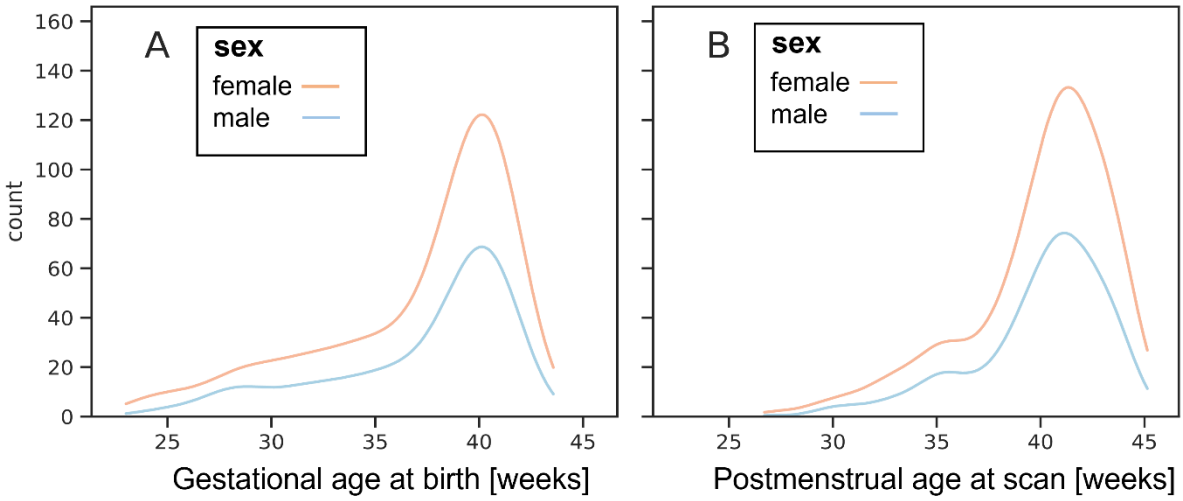

Figure 1. Histograms showing ages for boys and girls at (A) birth and (B) postnatal MR imaging

MR imaging data

Overview

A summary schematic of the imaging data flow is shown in figure 2 with further detail about the steps in the following section. This incorporated optimized MR acquisition sequences, novel image reconstruction methods, transfer to an intermediate server (InstaDB) prior to processing of the using state-of-the-art pipelines, and packaging of the data for final public release.

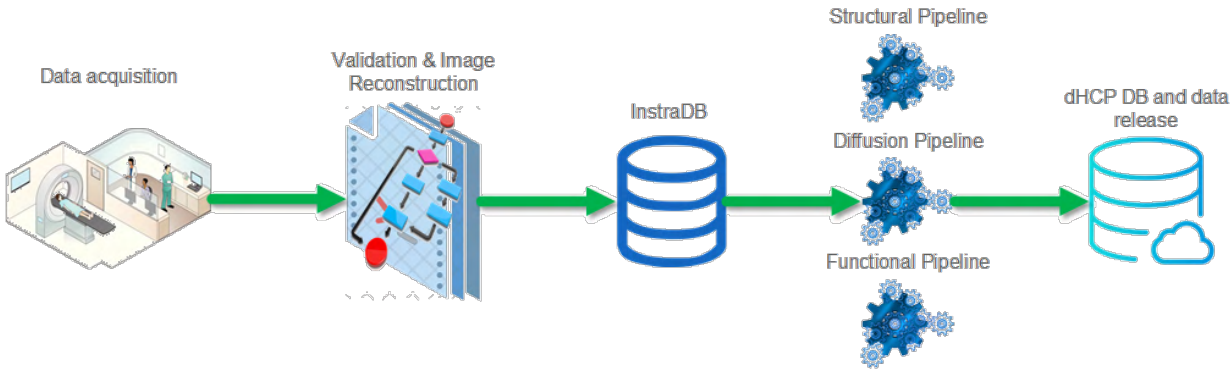

Figure 2. Schematic of the Developing Human Connectome Project imaging data flow from acquisition to data release.

The data release contains anatomical (T1 weighted (T1w) and T2 weighted (T2w)), resting state functional MRI (rsfMRI) and diffusion MRI (dMRI) images supplied as both original image data and after the processing pipelines described below have been applied.

The neonatal brain has significantly different tissue properties to the adult brain, including higher water content and incomplete myelination of white matter, and T1 and T2 relaxation times are generally longer than in the adult brain. Neonatal white matter in particular, has longer T1 and T2 times in comparison to grey matter, and brain anatomy is revealed more clearly on T2w images as there is greater contrast compared to T1w images. T2w images are thus treated as the primary data for anatomical segmentation and to provide the anatomical substrates for functional and diffusion analysis.

To ameliorate the effects of infants and fetuses moving during image acquisition novel neonatal patient handling and motion-tolerant acquisition approaches were developed (Cordero-Grande et al., 2020, Cordero-Grande et al., 2018, Hutter et al., 2018a, Hughes et al., 2017). Participants were imaged in natural sleep, with 6 exceptions who were sedated with chloral hydrate. If a baby woke up, scanning was halted and the infant settled without taking them out of the imaging cradle. However, as many infants still move even when sleeping peacefully, all subjects were motion corrected.

887 sessions are being released. 886 had T2w images that passed quality control (QC). 818 had fMRI data that passed QC and 758 had dMRI data that passed QC. Detailed information about the QC process are described in the notes accompanying the data release (https://biomedia.github.io/dHCP-release-notes/). The T1w images were not required by pre-processing pipelines and were placed at the end of the scanning protocol resulting in more variable quality than the T2w data; the release contains 711 sessions with T1w multi-slice fast spin-echo (FSE) images and 734 sessions with T1 3D magnetization-prepared rapid gradient-echo (MPRAGE) images.

Imaging acquisition methods and parameters

Imaging was carried out on a 3T Philips Achieva scanner running modified Release 3.2.2 software, using a dedicated neonatal imaging system which included a neonatal 32 channel phased array head coil and customized patient handling system (Rapid Biomedical GmbH) (Hughes et al., 2017). Infants were imaged following feeding and swaddling in a vacuum-evacuated blanket. Infants were provided with hearing protection in the form of: molded dental putty placed in the external auditory meatus (President Putty, Coltene Whaledent, Mahwah, NJ, USA); Minimuffs (Natus Medical Inc, San Carlos CA, USA); and an acoustic hood. Monitoring throughout the scanning session (Invivo Expression,

Philips, Best, NL), included pulse oximetry, respiration (using a small air cushion placed on the lower abdomen) and body temperature via a fiber optic probe placed in the axilla. The bespoke imaging cradle system (Hughes et al., 2017) placed subjects in a standardized pose and allowed a fixed imaging geometry to be deployed, with only the position in the head-foot direction adjusted at the start of the examination. The field of view was set after a biometric analysis of data from 91 previously studied term-born infants with dimensions sufficient to accommodate 95% of late-term neonates (Hughes et al., 2017).

To reduce the risk of waking infants due to startle responses at the start of new sequences, the scanner software was modified to ramp up the gradient waveforms gradually over 5 seconds as each acquisition commenced and prior to any radiofrequency (RF) pulses or data being acquired. Calibration scans, anatomical images (T1w and T2w), resting state functional (rs-fMRI) and diffusion (dMRI) acquisitions were acquired, with an average data rate of 27 slices/second including all preparation and calibration phases. The acquisition protocol was optimized for the properties of the neonatal brain and for efficiency and is summarized in table 1.

Sequence name	**Duration**	**Acquisition reference publications**	**Processing pipeline reference publications**
Pilot	00:00:10		
Coil reference	00:01:14		
B0 calibration map	00:00:20	(Gaspar et al., 2015)	
B1 map	00:00:05		
T2 Turbo Spin Echo (TSE) axial	00:03:12	(Hughes et al., 2017, Cordero-Grande et al., 2016, Cordero-Grande et al., 2018)	(Makropoulos et al., 2018, Schuh et al., 2017)
T1 MPRAGE	00:04:35		
T2 TSE sagittal	00:03:12		
Spin Echo (SE) fMRI ref.	00:01:53	(Price et al., *manuscript in preparation*)	(Baxter et al., 2019, Fitzgibbon et al., 2020)
Single-Band (SB) fMRI ref.	00:00:19		
Multi-Band (MB) fMRI	00:15:03		
SB fMRI ref. repeat	00:00:19		
SB diffusion MRI ref.	00:01:39	(Cordero-Grande et al., 2019, Cordero-Grande et al., 2018, Hutter et al., 2018a, Hutter et al., 2018b, Tournier et al., 2020)	(Bastiani et al., 2019, Christiaens et al., 2021, Pietsch et al., 2019, Christiaens et al., 2019)
MB diffusion MRI	00:19:20		
B0 shim map	00:00:20		

T1 TSE Inversion Recovery (IR) axial	00:05:45	(Cordero-Grande et al., 2018)	
T1 TSE IR sagittal	00:05:45		
Total	**01:03:11**		

Table 1: Neonatal imaging protocol, lasting a total of 1 hour 3 minutes 11 seconds

Sequence details were as follows:

Calibration scans: Static magnetic field (B0) mapping was performed using an interleaved dual TE spoiled gradient echo sequence and localised image-based shimming performed for use with all EPI sequences (Gaspar et al., 2015). Following application of optimized 1st and 2nd order shim settings, B0 (shimmed) field maps were acquired after the fMRI and dMRI acquisitions, and later in the cohort were acquired between the two acquisitions. B1 mapping was performed using the dual refocusing echo acquisition mode (DREAM) method (Nehrke and Bornert, 2012), with STE first and STEAM flip angle of 60.

Anatomical acquisition: Imaging parameters were optimized for contrast to noise ratio using a Cramer Rao Lower bound approach (Lankford and Does, 2013) with nominal relaxation parameter values for grey matter T1/T2: 1800/150ms and white matter T1/T2: 2500/250ms (Williams et al., 2005). T2w and inversion recovery T1w multi-slice FSE images were each acquired in sagittal and axial slice stacks with in-plane resolution 0.8x0.8mm^2 and 1.6mm slices overlapped by 0.8mm (except in T1w Sagittal which used a slice overlap of 0.74mm). Other parameters were – T2w: TR/TE=12000/156ms, SENSE factor 2.11 (axial) and 2.60 (sagittal); T1w: TR/TI/TE=4795/1740/8.7ms, SENSE factor 2.27 (axial) and 2.66 (sagittal). 3D MPRAGE images were acquired with 0.8mm isotropic resolution and parameters: TR/TI/TE=11/4.6/1400/4.6ms, SENSE factor 1.2 RL (Right-Left). The FSE acquisitions were each reconstructed using a motion correction algorithm and then the transverse and sagittal images were fused into a single 3D volume for each modality using slice-to-volume methods (Cordero-Grande et al., 2016).

rs-fMRI: A fMRI acquisition with high temporal resolution developed for neonates (Price et al *in preparation*) (Fitzgibbon et al., 2020) using multiband (MB) 9x accelerated echo-planar imaging was collected for 15 minutes, with parameters: TE/TR=38/392ms, 2300 volumes, with an acquired spatial resolution of 2.15mm isotropic. No in-plane acceleration or partial Fourier was used. Single-band

reference scans were also acquired with bandwidth matched readout, along with additional spin-echo acquisitions with both anterior-posterior/posterior-anterior (AP/PA) fold-over encoding directions. Physiological recordings of vectorcardiogram (VCG), photoplethysmogram (PPU) and respiratory traces during the fMRI data acquisition are provided unprocessed in the source data folder for optional physiological artifact removal. Alignment to rs-fMRI data can be achieved by means of locating the 'end of scan' marker (scripts are available to aid loading and interpretation of this file) and knowledge of the frequency of the recordings (496Hz) and TR x number of volumes acquired (0.392s x 2300) can be used to identify the start of scan timepoint. Note, for improved accuracy on this cohort a small delay of ~85ms between the true end of data acquisition and 'end of scan' marker has been identified. After accounting for this, the precision of identifying the true start of scan in the physiological file should be on the order of +/- 50ms, for a complete scan of 15 minutes duration.

dMRI: The dMRI acquisition was optimized for the properties of the developing brain (Tournier et al., 2020) and implemented as a uniformly distributed set of directions on 4 shells (b = 0 s/mm^2: 20, b = 400 s/mm^2: 64, b = 1000 s/mm^2: 88, b = 2600 s/mm^2: 128), each of which was split into 4 optimal subsets acquired using AP, PA, RL, and LR phase encoding (Hutter et al., 2018b). As described in (Hutter et al., 2018b), the diffusion gradient b-values and directions and the phase encoding directions were spread temporally taking the risk of infant motion and gradient duty cycle considerations into account in order to achieve maximal imaging efficiency. If the subject woke up during the diffusion scan, the acquisition could be halted and restarted (after resettling the subject) with a user defined overlap in acquired diffusion weightings. The EPI sequence uses MB factor 4, SENSE factor 1.2, partial Fourier factor 0.86, in-plane resolution 1.5x1.5mm, 3mm slices with 1.5mm overlap, TE=90ms, TR=3800ms. Image reconstruction used a dedicated SENSE algorithm (Cordero-Grande et al., 2018, Zhu et al., 2016, Hennel et al., 2016).

Processing pipelines

Standardized processing pipelines for all three MRI modalities (anatomical, diffusion and functional imaging) have been developed specifically for the dHCP neonatal data. The outputs of these pipelines are supplied as part of the data release. Details of the individual pipelines have been published elsewhere including: anatomical segmentations into 9 tissues and 87 regions, and extracted cortical surfaces (Makropoulos et al., 2018) and cortical atlases (Bozek et al., 2018), resting state fMRI analysis (Fitzgibbon et al., 2020) and two diffusion analysis pipelines based on FSL EDDY (Bastiani et al., 2019) and based on SHARD slice-to-volume reconstruction (Christiaens et al., 2021, Christiaens et al., 2019). The SHARD pipeline also includes de-noised source diffusion data (Cordero-Grande et al., 2019) and inter-slice intensity correction (Pietsch et al., 2021). These offer

natural entry points for those wishing to use image analysis software such as FSL (www.fmrib.ox.ac.uk/) and MRtrix3 (www.mrtrix.org) for further analysis. An atlas of diffusion properties has also been created based on a multi-shell multi-tissue constrained spherical deconvolution model (Pietsch et al., 2019). Whilst the majority of the processing pipelines are designed specifically for neonatal data given the inherent differences in tissue contrast and image properties, most analysis pipelines were also set up for comparison with adult data in mind. For instance, the cortical analysis pipeline was aligned with the young adult HCP FS_LR template space. However, we would urge caution about directly comparing adult and neonatal data given that much of the HCP dataset is aligned and parcellated using adult functional networks, and it is likely that the developing functional networks are not sufficiently developed to support this.

Exemplar imaging data

Figures 3 – 8 show examplar data for one participant to provide an indication of what is available. Figure 3 shows anatomical T1w and T2w fast spin echo data from this infant with the native images for all the acquisitions and the final motion corrected reconstructions. Although the infant was asleep, there is still some residual motion artifact. However, the final reconstruction can be seen to be of high quality after motion correction. The MPRAGE data (not shown) is not motion corrected, so is more vulnerable to subject motion. The anatomical segmentation into tissue type and neonatal brain atlas regions are shown in Figure 4, and cortical surfaces with projection of the atlas and example derived measures for this subject are shown in Figure 5. Anatomical atlases at one week intervals are available for download (https://brain-development.org/brain-atlases/atlases-from-the-dhcp-project/) and will also be available from the NIMH database (https://nda.nih.gov/edit_collection.html?id=3955). Figure 6 shows one volume of the fMRI time series and a single subject network analysis from the pipeline. Figures 7 and 8 show diffusion data. Figure 7 shows selected images from all shells, before correction, after denoising, and after motion and distortion correction and destriping (Pietsch et al., 2021). Figure 8 shows derived dMRI metrics in the same slice, including the mean diffusivity (8a) and fractional anisotropy (8b) of the diffusion tensor (Basser et al., 1994), fibre orientation distribution functions (8c) estimated using multi-component spherical deconvolution (Jeurissen et al., 2014, Pietsch et al., 2019) produced with MRtrix3 (Tournier et al., 2019), and (9d) whole brain probabilistic streamline tractography using all tissue components and using only the mature white matter like component from the neonatal multi-component model (Pietsch et al., 2019).

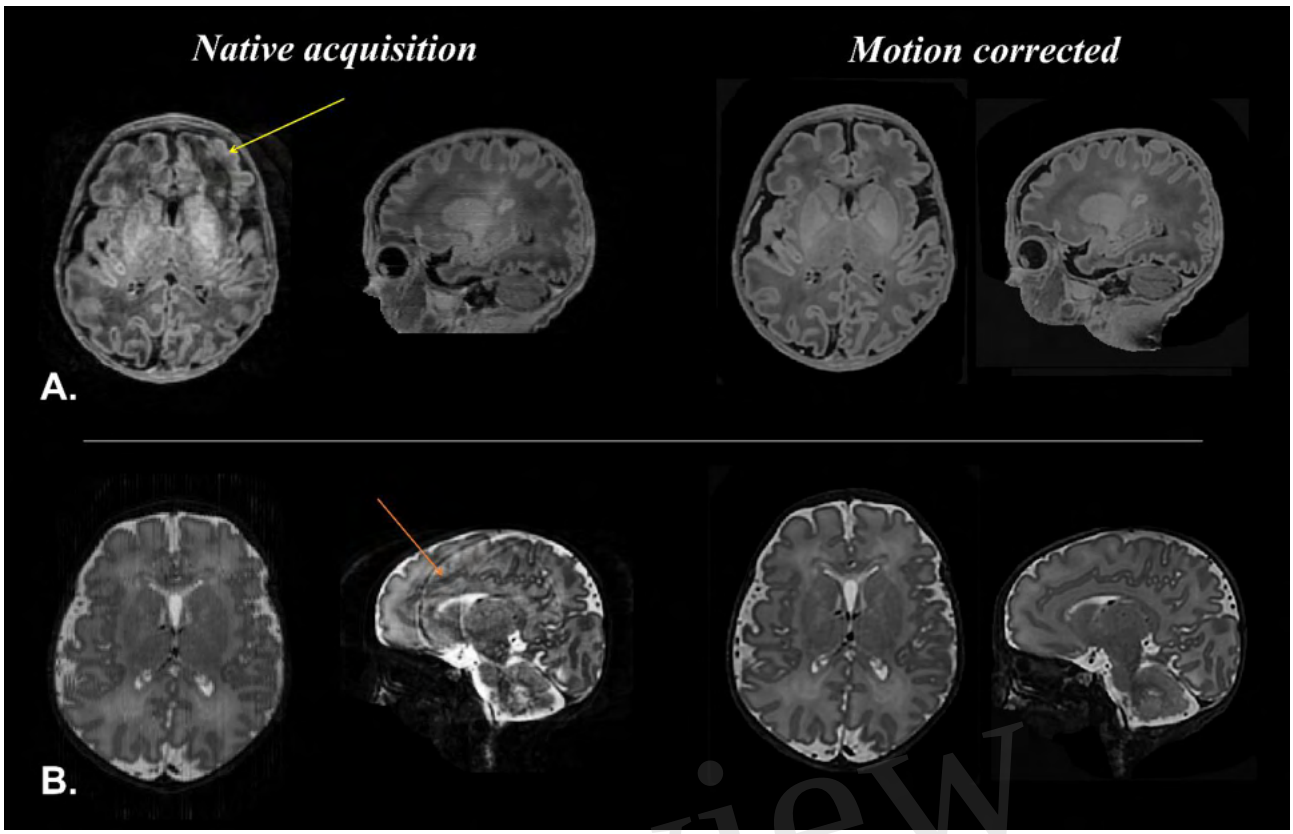

Figure 3. Anatomical T1 and T2 weighted images before and after motion correction for one participant. A. (top row) T1 native acquisition (left) with motion artefact visible in the left frontal region in the transverse plane (yellow arrow), which is resolved in the motion corrected images (right) after slice to volume reconstruction. B. (bottom row) T2 native acquisition (left) with motion artefact visible in the sagittal plane (orange arrow), which is resolved in the motion corrected images (right).

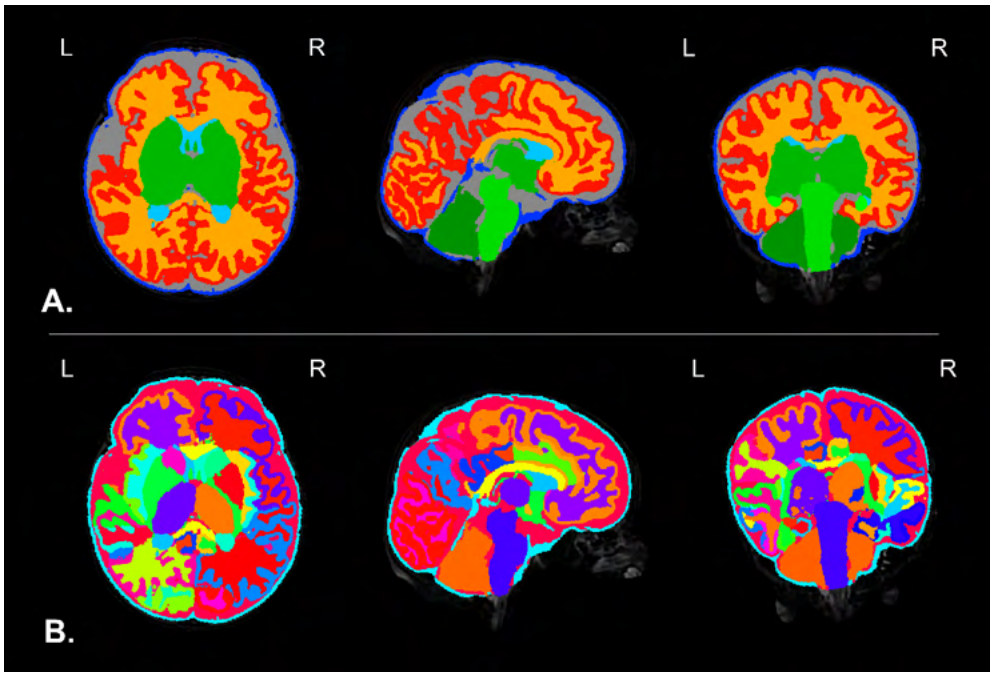

Figure 4. Tissue segmentation and neonatal atlas parcellation for the same infant. Using the automated dHCP structural pipeline, the anatomical images can be segmented into 9 tissue classes (A. top row) and parcellated into 87 brain regions (B. bottom row).

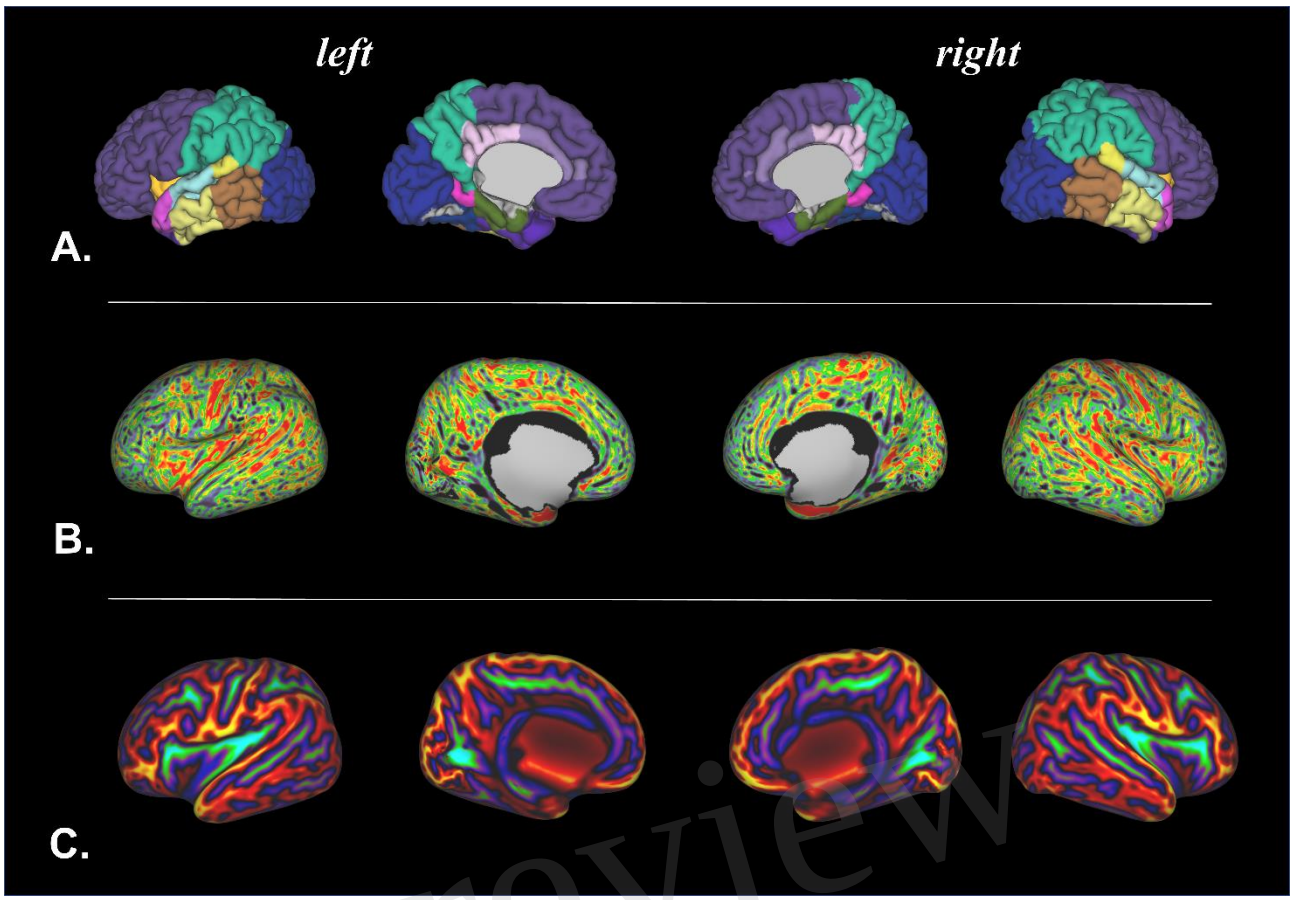

Figure 5: Surface projections using the dHCP structural pipeline for the same infant. A. (top row) 87 region neonatal brain atlas projected onto the pial surface; B. (middle row) cortical thickness projected onto the inflated cortical surface; and C. (bottom row) sulcal depth projected onto the inflated cortical surface.

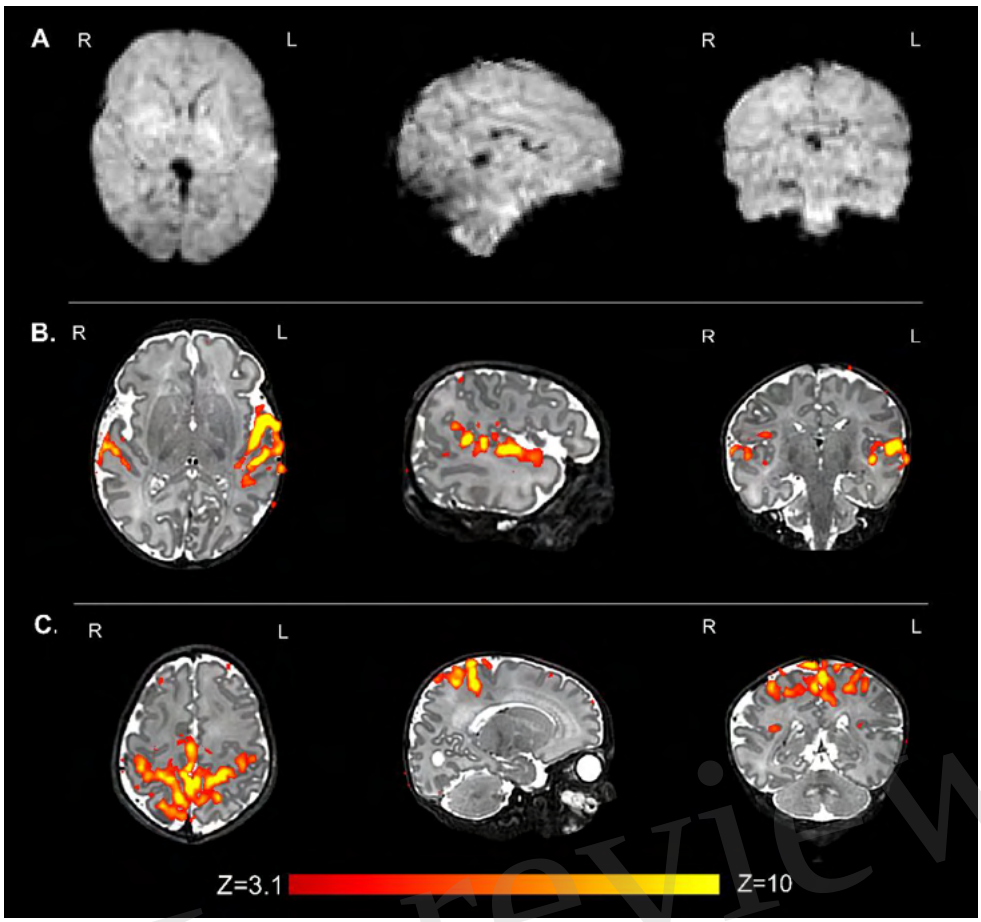

Figure 6. Resting state functional MRI data from the same infant. A. an example volume from the fMRI acquisition after image reconstruction and the preprocessing pipeline has been applied; and B. the auditory and C. sensorimotor resting state networks. Resting state networks were defined using independent component analysis (ICA) as implemented in FSL MELODIC and have been overlaid onto the native T2 image for ease of visualization.

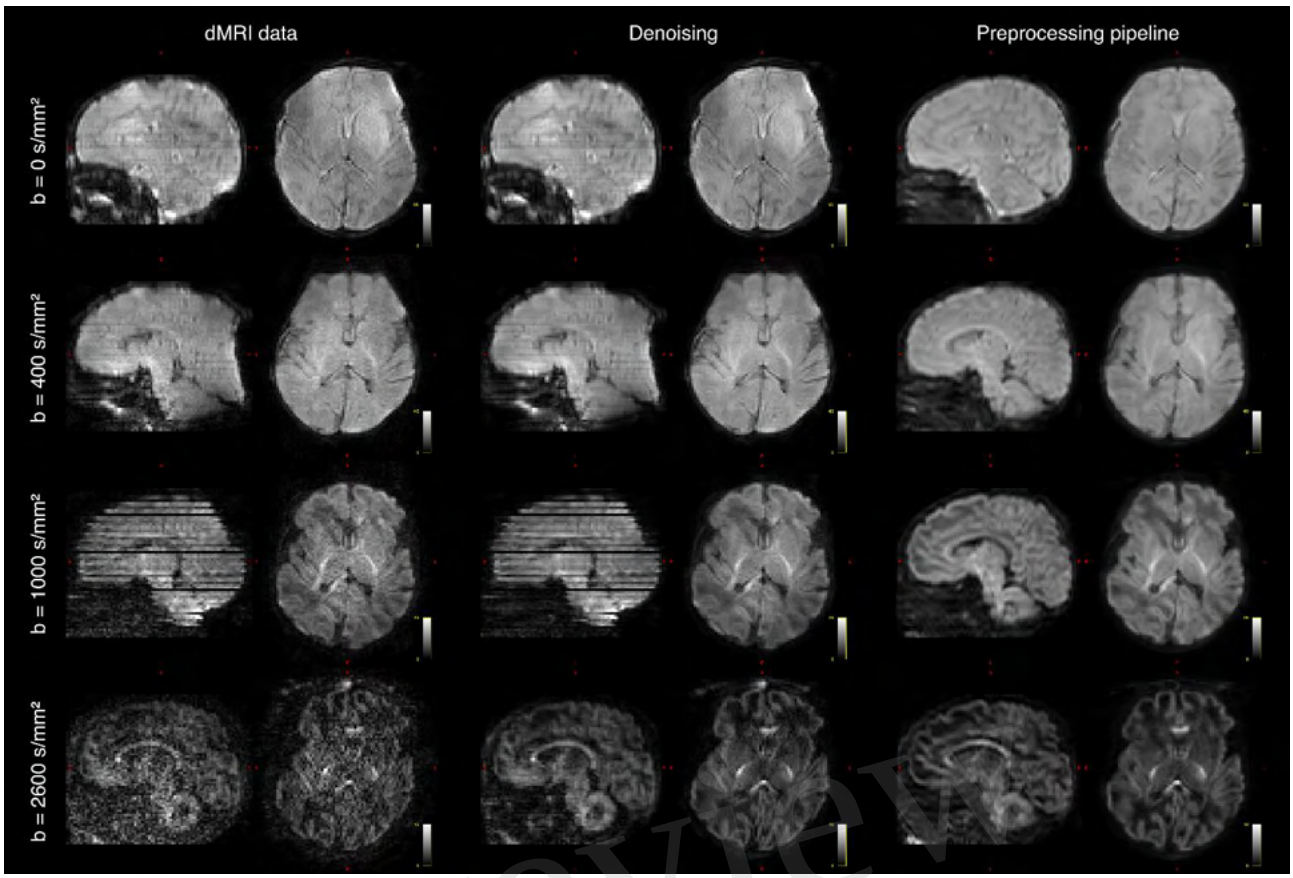

Figure 7. Diffusion MRI (dMRI) data from the same infant. Shown are 4 selected volumes with different *b*-values and phase encoding directions. Left: input data after MB-SENSE reconstruction. Middle: images after denoising. Right: images after motion and distortion correction and destriping.

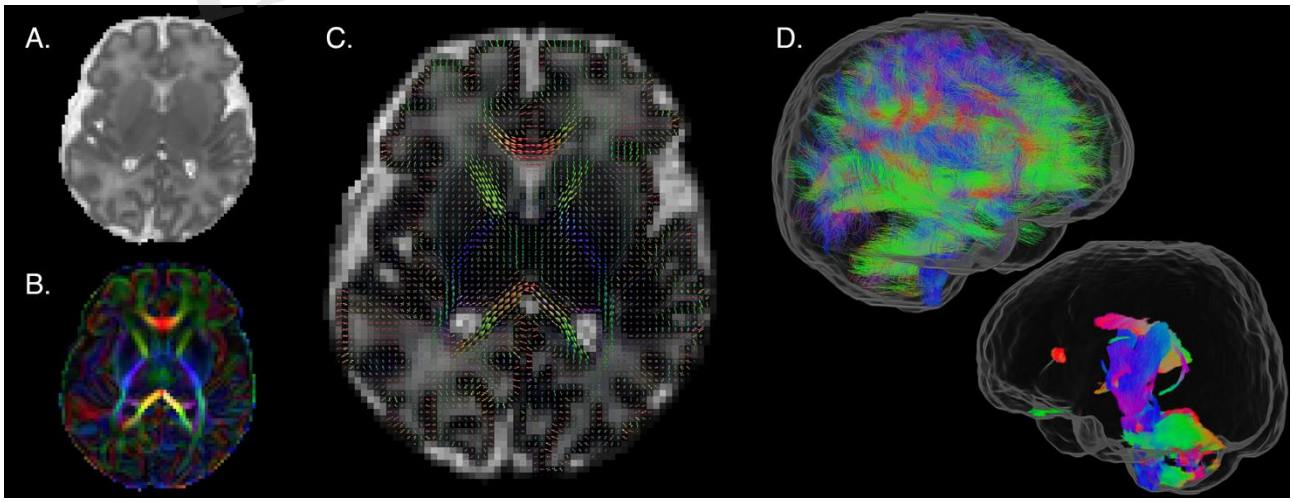

Figure 8. dMRI metrics in a single subject from the same infant (A) Mean Diffusivity and (B) Color Fractional Anisotropy maps of the Diffusion Tensor Imaging (DTI) model. (C) Tissue Orientation Distribution Function (ODF) of the multi-component analysis in Pietsch et al. (2019). (D) Full brain probabilistic streamline tractography based on the tissue ODF (top image) and based on the mature appearing tissue component (bottom image).

Collateral Data

A broad spread of demographic and other data is available, although practical constraints, including the COVID-19 pandemic, have led to a certain amount of missing data. The data codebook can currently be accessed through the dHCP website (www.developingconnectome.org) and NIMH database (https://nda.nih.gov/edit_collection.html?id=3955), providing a listing with descriptions of the variables. The data sets include the following categories of data.

Demographic, Family and Clinical data.

Demographic Data for Parents: age at conception; ethnicity according to UK census categories; highest age enrolled in full-time education; occupation. This data is collected at enrolment and again at the 18-month neurodevelopmental assessment.

Mother's past medical history: height, weight, body mass index (BMI); blood group; history of medical conditions prior to the pregnancy; smoking, alcohol, and recreational drug use; injury during the pregnancy.

Mother's obstetric history: previous pregnancies; number of live births; number of miscarriages; previous premature birth; current pregnancy type, mode of conception (natural or IVF); pregnancy number; late pregnancy and labour/delivery history for the pregnancy.

Mental health history: self-reported by mother at enrolment and self-reported by both parents at the 18-month assessment, including any history of parental psychiatric problems and how treated; parental history of attention deficit hyperactivity disorder (ADHD), bipolar disease, autistic spectrum disorder (ASD) or schizophrenia; ASD or ADHD in proband's siblings; close relatives with history of ASD, ADHD, bipolar disease, or schizophrenia.

Baby medical details at birth: gestational age at birth; birth weight, length and occipito-frontal head circumference; presentation and mode of delivery; medication required at delivery, nutrition and feeding; Apgar scores at 1 and 5 minutes of age; arterial cord blood pH and base excess where available. The majority of dHCP participants were born in good health and were not admitted to the neonatal intensive care unit (NICU), for those who were, summary data for each day on the neonatal unit and an overall summary of the stay are recorded.

Neurodevelopmental and Neurocognitive testing at 18 months

A series of standardized age-appropriate child-centred assessments, parent-report questionnaires and gaze-tracking tasks were used to provide a targeted overview of toddlers' development. These measures were chosen to be able capture individual differences along a typical-to-atypical continuum, to probe associations between early imaging features and emerging behavioural outcomes and to provide normative reference data for future studies.

619 infants (79%) attended for follow-up assessment, planned for 18 months corrected age but affected by the COVID-19 pandemic, so that median (range) of assessment was 18 months + 12 days (range 17 + 8 – 34 + 15). Completion rates for broad components of this assessment are shown in tables 2 and 3.

Neurodevelopmental assessment/Questionnaire	**Number (%)**
Bayley III Cognitive, language, motor neurodevelopmental variables	602 (77%)
Neurological examination total score	594 (76%)
Early Childhood Behavioral Questionnaire (ECBQ)	592 (76%)
Child Behavioral Checklist (CBCL)	591 (76%)
Quantitative Checklist for Autism in Toddlers (Q-CHAT)	591 (76%)
Cognitively Stimulating Parenting Scale (CSPS)	583 (75%)
Parenting Scale: primary caregivers' laxness, over reactivity, verbosity	589 (75%)
Parenting Scale: secondary caregivers' laxness, over reactivity, verbosity	517 (66%)

Table 2: Completion rates for neurodevelopmental assessments and questionnaires.

The Bayley Scales of Infant and Toddler Development, Third Edition (Bayley-III): assessed toddlers' cognitive, language (receptive and expressive) and motor abilities (gross and fine) using age normed standardized scores (mean = 100, SD = 15) (Albers and Grieve, 2007). The age of assessment and distribution of Bayley III cognitive scores for boys and girls are shown in Figure 9.

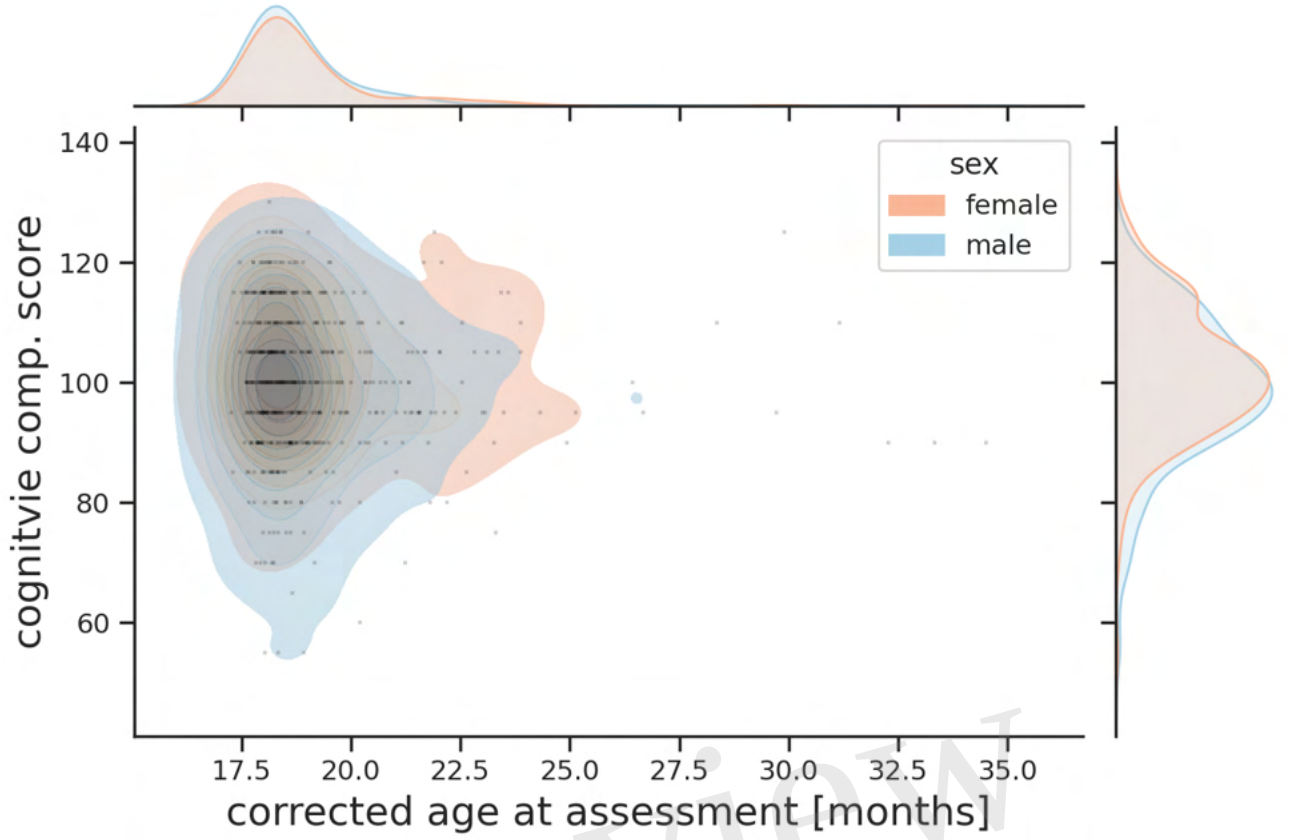

Figure 9. Probability plot showing age of assessment and combined Bayley III cognitive score for boys and girls.

The Neurological Examination of Infant/Child: used 26 non-age dependent items to assess cranial nerve function, posture, movements, tone and reflexes (Haataja et al., 1999).

Behavioural questionnaires completed by primary caregivers

Early Childhood Behaviour Questionnaire (ECBQ): this measures dimensions of temperament, referring to individual differences in reactivity and self-regulation (Putnam and Rothbart, 2006). The ECBQ describes three broad scales: Surgency, characterized by impulsivity, intense pleasure seeking and high activity levels; Negative Affectivity, which refers to the disposition to experience aversive affective states, such as anger, fear, anxiety, shame and disgust; Effortful Control, which refers to the capacity to inhibit/activate a behavioural response by focusing attention.

Child Behavioral Checklist for Ages 1.5 to 5 (CBCL): which is a 100-item measure on the frequency of behavioral and emotional problems in young children (Achenbach and Ruffle, 2000). The CBCL yields scores for seven problem behavior syndrome subscales: Emotionally Reactive, Anxious/ Depressed, Somatic Complaints, Withdrawn, Sleep Problems, Attention Problems, and

Aggressive Behaviour. Scores are also derived for Externalizing Problems, Internalizing Problems and Total Problems.

Quantitative Checklist for Autism in Toddlers (Q-CHAT): a 25-item questionnaire designed to assess potential autistic traits in children (Allison et al., 2008).

Cognitively Stimulating Parenting Scale (CSPS): adapted from (Wolke et al., 2013), which assesses the availability and variety of experiences that promote cognitive stimulation in the home. This includes availability of educational toys, parental interactions such as teaching words or reading stories, and cognitively stimulating activities such as family excursions. The version of the CSPS used here was updated to include four items now widely used by toddlers (i.e., iPhone and Apps) (Bonthrone et al., 2021). Scores from the 28 items included in the CSPS can be aggregated to provide an overall cognitively stimulating parenting score.

Parenting Scale: is a 30-item rating scale that measures dysfunctional parenting in discipline situations (Arnold et al., 1993). Parents are asked to indicate their tendency to use specific discipline practices using a 7-point scale. The Parenting Scale identifies three different suboptimal parenting styles, as well as a total score providing a dysfunctional parenting index. Over-reactivity indicates authoritarian and coercive discipline practices; Laxness, in contrast, describes a permissive parent who is inconsistent in providing discipline; Verbosity refers to a parenting style characterized by lengthy and ineffective verbal reprimands. Primary carers were usually mothers and secondary carers usually fathers.

Eye-tracking: used to obtain data on a number of cognitive processes. The Tobii TX-300 (Tobii AB, Sweden) gaze tracking system was used to record the temporal and spatial features of the children's direction of gaze in 609 infants (78%) at a median age of 18 months + 12days (range 17+ 8 – 34 + 15). The battery of tasks comprised a series of animated video clips designed to measure endogenous and exogenous visual attention (Elsabbagh et al., 2013, Elsabbagh et al., 2009, Gliga et al., 2009, Wass et al., 2011). Extracted metrics included visual engagement and disengagement, efficiency of attention shifting, social and non-social attention and memory guided choices and visual search. The list of tests and completion rates are shown in table 3. A manuscript describing the tasks and the results in detail has been submitted for publication (Braithewaite, Kyriakopoulou et al, *submmitted*). The project codebook details the variables to be released, while the rich meta-data from these tests may be available through discussion with the dHCP investigators.

Eye-tracking task	**N (%)**
Gap-overlap	602 (77)

Non-social contingency	597 (76)
Visual search	597 (76)
Fishtanks	596 (76)
Cognitive control	585 (75)
Working memory	585 (75)
Emotions	576 (74)
Smooth pursuit fixation	568 (72)
Fixation	484 (64)
Scenes	483 (61)
Static images	481 (61)
Entire eye-tracking battery completed	453 (58)

Table 3. Tests and completion rates for eye tracking assessments

Genomic Data

Genetic data: Saliva samples were collected at the initial neonatal MRI data acquisition and 18-month old infant timepoints using Oragene DNA OG-250 kits (DNAGenotek Inc., Kanata, Canada). The genotyping was performed on only one sample (usually the first). There are no linked maternal or paternal samples. Samples were genotyped on the Illumina Infinium Omni5-4 array v1.2, which comprises a total of 4327108 SNPs, by NIHR BioResource Centre Maudsley Genomics & Biomarker Core Facility. Genotyping was undertaken in two batches. Basic quality control was performed by the Department of Biostatistics & Health Informatics, King's College London for the combined dHCP batches and a small additional independent study cohort. Raw Illumina microarray genotype image (IDAT) files were uploaded into GenomeStudio and processed according to the GenomeStudio quality control Standard Operating Procedure (https://khp-informatics.github.io/COPILOT/index.html). Data was then further processed according to an in-house pipeline which identified and removed samples with call rates below 95%. It also identified gender mismatches and potential heterozygosity outliers which are flagged in the metadata files. SNP data are available for 731 infants.

Methylation Data: Saliva-derived DNA from each sample was treated with sodium bisulfite (Zymo Research EZ-96 DNA Methylation Kit (D5004)). DNA methylation was quantified using the Illumina Infinium HumanMethylationEPIC BeadChip Kit. Methylation analysis for the dHCP samples was undertaken alongside two additional independent study cohorts. A randomized sample layout was generated using key study parameters including all study cohorts, with Omixer R/Bioconductor package (http://www.bioconductor.org/packages/release/bioc/html/Omixer.html). Saliva samples

have been processed for 739 infants, including a subset with samples taken at birth and repeated at the 18-month visit, but QC has yet to be carried out.

Governance and Access

The study was approved by the UK Health Research Authority (Research Ethics Committee reference number: 14/LO/1169) and written parental consent was obtained in every case for imaging and open data release of the anonymized data. The main imaging data, essential metadata and the collateral data, will be available after accepting a data sharing agreement. Downloaded data should not be passed on to third parties outside the research group, and no attempt should be made to de-anonymize the data which have been face stripped to prevent attempts at facial recognition.

The preliminary data releases are currently available to download by academic torrent via the dHCP website (www.developingconnectome.org). The primary long-term site for curation and access of the full data release will be the National Institute for Mental Health (NIMH) data repository portal at https://nda.nih.gov/edit_collection.html?id=3955.

Examples of dHCP data use

The preliminary data releases of a proportion of the images have been available to scientists since 2019. There datasets have been accessed frequently and already a large number of studies have been published using dHCP data. These include studies of prenatal opioid exposure (Merhar et al., 2021), cerebral gene expression (Ball et al., 2020), the effects of preterm birth on brain structure and function (Dimitrova et al., 2020, Kline et al., 2020, Eyre et al., 2021), the development of specific cognitive functions (Li et al., 2020), and the neural response to noxious stimuli (Baxter et al., 2019), as well as a number of analyses of brain connectivity and growth (Eyre et al., 2021, Wang et al., 2021, Bethlehem et al., 2022). The data have been widely used to develop novel imaging analytic methods (Collins-Jones et al., 2021, Ding et al., 2020, Grigorescu et al., 2021) and to define new approaches to understanding brain development (Adamson et al., 2020, O'Muircheartaigh et al., 2020).

Discussion

We describe here the main neonatal data release of the Developing Human Connectome Project which includes 887 datasets from 783 subjects. We are releasing data from all steps in the project, from the initial images through intermediate steps in processing, to results from running our processing pipelines. The aim is to allow researchers to work with the data as they wish, without pre-filtering the

available selection. In the majority of cases high quality images across all modalities are available, and are linked to rich collateral data, although practical issues, notably the COVID-19 pandemic, led to some incomplete ascertainment.

Each image acquisition that contributes to the dHCP collection was individually optimized both to take account of the properties of the developing neonatal brain and to achieve the most efficient total examination. After the initial piloting in which the head-foot location of the imaging volume was set, the scanner operated without pause for the entire examination.

Virtually all subjects were examined during natural sleep, so available time for imaging was constrained. We took steps to reduce the risk that infants would awaken by minimizing preparation time after feeding was complete, improving the patient-handling equipment (see (Hughes et al., 2017) for details) and modifying the scanner software to avoid sudden changes in acoustic conditions that might create a startle response. Despite these precautions some babies did wake up during the scanning session, but it was often possible to re-settle them and the protocol was designed to allow restart with minimal time penalty, particularly for the dMRI, which was the longest single acquisition. Although precise information about whether a baby woke up during image acquisition was not recorded, it would be of interest in future studies exploring the specific relationship between imaging measures and behavior.

However, even those babies that continued to sleep often moved sufficiently to impair the data quality of the advanced images being collected, so data were motion corrected, either as part of a motion corrected image reconstruction (Anatomical T2w and T1w FSE sequences, but not MPRAGE) or as part of the data processing pipelines, each of which had motion correction steps included. These pipelines were designed and optimized specifically for neonatal data, and software for pipelines is freely available (https://biomedia.github.io/dHCP-release-notes/open-resources.html). Full details are available as part of the data download documentation.

The data from the dHCP naturally sits within a context of other connectome-oriented collections and will be curated alongside many similar resources by the National Institutes of Mental Health in the large multimodal neuroinformatic data repository. The dHCP neonatal data collection will prove valuable to a broad range of users and that it will complement and augment other available materials. Taken together with the dHCP fetal data release, this collection provides what is currently a unique observational resource that captures information on the developing human brain at a key stage of rapid growth and change. The companion genetic and follow-up behavioural resources, as well as

atlases, which will be accessed from the same locations, can provide rich materials to address a range of scientific and clinical questions. The data are already being widely used.

ACKNOWLEDGMENTS

We are grateful for all the families who kindly agreed to participate in the project and recognise their particular commitment in remaining engaged with the programme during the COVID-19 Pandemic. We also acknowledge the support of the Neonatal Intensive Care Unit and the Newborn Imaging Centre at Evelina London Children's Hospital.

The Developing Human Connectome Project was funded by the European Research Council under the European Union Seventh Framework Programme (FP/20072013)/ERC Grant Agreement no. 319456. The work was supported by: the NIHR Biomedical Research Centres at Guys and St Thomas NHS Trust and the South London and Maudsley NHS Trust; the ESPRC/Wellcome Centre for Medical Engineering; and the MRC Centre for Neurodevelopmental Disorders.

TA is supported by a MRC Clinician Scientist Fellowship [MR/P008712/1] and MRC translation support award [MR/V036874/1]. JOM is supported by a Sir Henry Dale Fellowship jointly funded by the Wellcome Trust and the Royal Society [Grant Number 206675/Z/17/Z].

REFERENCES

Achenbach, T. M. & Ruffle, T. M. 2000. The Child Behavior Checklist and related forms for assessing behavioral/emotional problems and competencies. *Pediatr Rev,* 21**,** 265-71.

Adamson, C. L., Alexander, B., Ball, G., Beare, R., Cheong, J. L. Y., Spittle, A. J., et al. 2020. Parcellation of the neonatal cortex using Surface-based Melbourne Children's Regional Infant Brain atlases (M-CRIB-S). *Sci Rep,* 10**,** 4359.

Albers, C. A. & Grieve, A. J. 2007. Test Review: Bayley, N. (2006). Bayley Scales of Infant and Toddler Development– Third Edition. San Antonio, TX: Harcourt Assessment. *Journal of Psychoeducational Assessment,* 25**,** 180-190.

Alexander-Bloch, A., Giedd, J. N. & Bullmore, E. 2013. Imaging structural co-variance between human brain regions. *Nat Rev Neurosci,* 14**,** 322-36.

Allison, C., Baron-Cohen, S., Wheelwright, S., Charman, T., Richler, J., Pasco, G., et al. 2008. The Q-CHAT (Quantitative CHecklist for Autism in Toddlers): a normally distributed quantitative measure of autistic traits at 18-24 months of age: preliminary report. *J Autism Dev Disord,* 38**,** 1414-25.

Arnold, D. S., O'leary, S. G., Wolff, L. S. & Acker, M. M. 1993. The Parenting Scale: A measure of dysfunctional parenting in discipline situations. *Psychological Assessment,* 5**,** 137-144.

Ball, G., Seidlitz, J., O'muircheartaigh, J., Dimitrova, R., Fenchel, D., Makropoulos, A., et al. 2020. Cortical morphology at birth reflects spatiotemporal patterns of gene expression in the fetal human brain. *PLoS Biol,* 18**,** e3000976.

Bastiani, M., Andersson, J. L. R., Cordero-Grande, L., Murgasova, M., Hutter, J., Price, A. N., et al. 2019. Automated processing pipeline for neonatal diffusion MRI in the developing Human Connectome Project. *Neuroimage,* 185**,** 750-763.

Batalle, D., Edwards, A. D. & O'muircheartaigh, J. 2018. Annual Research Review: Not just a small adult brain: understanding later neurodevelopment through imaging the neonatal brain. *J Child Psychol Psychiatry,* 59**,** 350-371.

Baxter, L., Fitzgibbon, S., Moultrie, F., Goksan, S., Jenkinson, M., Smith, S., et al. 2019. Optimising neonatal fMRI data analysis: Design and validation of an extended dHCP preprocessing pipeline to characterise noxious-evoked brain activity in infants. *Neuroimage,* 186**,** 286-300.

Bethlehem, R. a. I., Seidlitz, J., White, S. R., Vogel, J. W., Anderson, K. M., Adamson, C., et al. 2022. Brain charts for the human lifespan. *Nature*, doi: 10.1038/s41586-022-04554-y.

Bonthrone, A. F., Chew, A., Kelly, C. J., Almedom, L., Simpson, J., Victor, S., et al. 2021. Cognitive function in toddlers with congenital heart disease: The impact of a stimulating home environment. *Infancy,* 26**,** 184-199.

Bozek, J., Makropoulos, A., Schuh, A., Fitzgibbon, S., Wright, R., Glasser, M. F., et al. 2018. Construction of a neonatal cortical surface atlas using Multimodal Surface Matching in the Developing Human Connectome Project. *Neuroimage,* 179**,** 11-29.

Carney, O., Hughes, E., Tusor, N., Dimitrova, R., Arulkumaran, S., Baruteau, K. P., et al. 2021. Incidental findings on brain MR imaging of asymptomatic term neonates in the Developing Human Connectome Project. *EClinicalMedicine,* 38**,** 100984.

Christiaens, D., Cordero-Grande, L., Hutter, J., Price, A. N., Deprez, M., Hajnal, J. V., et al. 2019. Learning Compact q -Space Representations for Multi-Shell Diffusion-Weighted MRI. *IEEE Trans Med Imaging,* 38**,** 834-843.

Christiaens, D., Cordero-Grande, L., Pietsch, M., Hutter, J., Price, A. N., Hughes, E. J., et al. 2021. Scattered slice SHARD reconstruction for motion correction in multi-shell diffusion MRI. *Neuroimage,* 225**,** 117437.

Collins-Jones, L. H., Arichi, T., Poppe, T., Billing, A., Xiao, J., Fabrizi, L., et al. 2021. Construction and validation of a database of head models for functional imaging of the neonatal brain. *Hum Brain Mapp,* 42**,** 567-586.

Cordero-Grande, L., Christiaens, D., Hutter, J., Price, A. N. & Hajnal, J. V. 2019. Complex diffusion-weighted image estimation via matrix recovery under general noise models. *Neuroimage,* 200**,** 391-404.

Cordero-Grande, L., Ferrazzi, G., Teixeira, R., O'muircheartaigh, J., Price, A. N. & Hajnal, J. V. 2020. Motion-corrected MRI with DISORDER: Distributed and incoherent sample orders for reconstruction deblurring using encoding redundancy. *Magn Reson Med*.

Cordero-Grande, L., Hughes, E. J., Hutter, J., Price, A. N. & Hajnal, J. V. 2018. Three-dimensional motion corrected sensitivity encoding reconstruction for multi-shot multi-slice MRI: Application to neonatal brain imaging. *Magn Reson Med,* 79**,** 1365-1376.

Cordero-Grande, L., Teixeira, R. P. a. G., Hughes, E. J., Hutter, J., Price, A. N. & Hajnal, J. V. 2016. Sensitivity Encoding for Aligned Multishot Magnetic Resonance Reconstruction. *IEEE Transactions on Computational Imaging,* 2**,** 266-280.

Craddock, R. C., Jbabdi, S., Yan, C. G., Vogelstein, J. T., Castellanos, F. X., Di Martino, A., et al. 2013. Imaging human connectomes at the macroscale. *Nat Methods,* 10**,** 524-39.

Dimitrova, R., Pietsch, M., Christiaens, D., Ciarrusta, J., Wolfers, T., Batalle, D., et al. 2020. Heterogeneity in Brain Microstructural Development Following Preterm Birth. *Cereb Cortex,* 30**,** 4800-4810.

Ding, Y., Acosta, R., Enguix, V., Suffren, S., Ortmann, J., Luck, D., et al. 2020. Using Deep Convolutional Neural Networks for Neonatal Brain Image Segmentation. *Front Neurosci,* 14**,** 207.

Elsabbagh, M., Gliga, T., Pickles, A., Hudry, K., Charman, T., Johnson, M. H., et al. 2013. The development of face orienting mechanisms in infants at-risk for autism. *Behav Brain Res,* 251**,** 147-54.

Elsabbagh, M., Volein, A., Holmboe, K., Tucker, L., Csibra, G., Baron-Cohen, S., et al. 2009. Visual orienting in the early broader autism phenotype: disengagement and facilitation. *J Child Psychol Psychiatry,* 50**,** 637-42.

Eyre, M., Fitzgibbon, S. P., Ciarrusta, J., Cordero-Grande, L., Price, A. N., Poppe, T., et al. 2021. The Developing Human Connectome Project: typical and disrupted perinatal functional connectivity. *Brain,* 144**,** 2199-2213.

Fitzgibbon, S. P., Harrison, S. J., Jenkinson, M., Baxter, L., Robinson, E. C., Bastiani, M., et al. 2020. The developing Human Connectome Project (dHCP) automated resting-state functional processing framework for newborn infants. *Neuroimage***,** 117303.

Gaspar, A. S., Price, A. N. & Nunes, R. G. 2015. Improving foetal and neonatal echo-planar imaging with image-based shimming. *Tese de mestrado integrado em Engenharia Biomédica e Biofísica, Universidade de Lisboa.* .

Gliga, T., Elsabbagh, M., Andravizou, A. & Johnson, M. 2009. Faces Attract Infants' Attention in Complex Displays. *Infancy,* 14**,** 550-562.

Grigorescu, I., Vanes, L., Uus, A., Batalle, D., Cordero-Grande, L., Nosarti, C., et al. 2021. Harmonized Segmentation of Neonatal Brain MRI. *Front Neurosci,* 15**,** 662005.

Haataja, L., Mercuri, E., Regev, R., Cowan, F., Rutherford, M., Dubowitz, V., et al. 1999. Optimality score for the neurologic examination of the infant at 12 and 18 months of age. *J Pediatr,* 135**,** 153-61.

Hennel, F., Buehrer, M., Von Deuster, C., Seuven, A. & Pruessmann, K. P. 2016. SENSE reconstruction for multiband EPI including slice-dependent N/2 ghost correction. *Magn Reson Med,* 76**,** 873-9.

Hisle-Gorman, E., Susi, A., Stokes, T., Gorman, G., Erdie-Lalena, C. & Nylund, C. M. 2018. Prenatal, perinatal, and neonatal risk factors of autism spectrum disorder. *Pediatr Res,* 84**,** 190-198.

Hughes, E. J., Winchman, T., Padormo, F., Teixeira, R., Wurie, J., Sharma, M., et al. 2017. A dedicated neonatal brain imaging system. *Magn Reson Med,* 78**,** 794-804.

Hutter, J., Christiaens, D. J., Schneider, T., Cordero-Grande, L., Slator, P. J., Deprez, M., et al. 2018a. Slice-level diffusion encoding for motion and distortion correction. *Med Image Anal,* 48**,** 214-229.

Hutter, J., Tournier, J. D., Price, A. N., Cordero-Grande, L., Hughes, E. J., Malik, S., et al. 2018b. Time-efficient and flexible design of optimized multishell HARDI diffusion. *Magn Reson Med,* 79**,** 1276-1292.

Jeurissen, B., Tournier, J. D., Dhollander, T., Connelly, A. & Sijbers, J. 2014. Multi-tissue constrained spherical deconvolution for improved analysis of multi-shell diffusion MRI data. *Neuroimage,* 103**,** 411-426.

Kline, J. E., Illapani, V. S. P., He, L., Altaye, M., Logan, J. W. & Parikh, N. A. 2020. Early cortical maturation predicts neurodevelopment in very preterm infants. *Arch Dis Child Fetal Neonatal Ed,* 105**,** 460-465.

Lankford, C. L. & Does, M. D. 2013. On the inherent precision of mcDESPOT. *Magn Reson Med,* 69**,** 127-36.

Li, J., Osher, D. E., Hansen, H. A. & Saygin, Z. M. 2020. Innate connectivity patterns drive the development of the visual word form area. *Sci Rep,* 10**,** 18039.
Makropoulos, A., Robinson, E. C., Schuh, A., Wright, R., Fitzgibbon, S., Bozek, J., et al. 2018. The developing human connectome project: A minimal processing pipeline for neonatal cortical surface reconstruction. *Neuroimage,* 173**,** 88-112.
Merhar, S. L., Kline, J. E., Braimah, A., Kline-Fath, B. M., Tkach, J. A., Altaye, M., et al. 2021. Prenatal opioid exposure is associated with smaller brain volumes in multiple regions. *Pediatr Res,* 90**,** 397-402.
Montagna, A. & Nosarti, C. 2016. Socio-Emotional Development Following Very Preterm Birth: Pathways to Psychopathology. *Front Psychol,* 7**,** 80.
Nehrke, K. & Bornert, P. 2012. DREAM--a novel approach for robust, ultrafast, multislice B(1) mapping. *Magn Reson Med,* 68**,** 1517-26.
O'muircheartaigh, J., Robinson, E., Pietsch, M., Wolfers, T., Aljabar, P., Grande, L. C., et al. 2020. Modelling brain development to detect white matter injury in term and preterm born neonates. *Brain,* 143**,** 467-479.
Pietsch, M., Christiaens, D., Hajnal, J. V. & Tournier, J. D. 2021. dStripe: Slice artefact correction in diffusion MRI via constrained neural network. *Med Image Anal,* 74**,** 102255.
Pietsch, M., Christiaens, D., Hutter, J., Cordero-Grande, L., Price, A. N., Hughes, E., et al. 2019. A framework for multi-component analysis of diffusion MRI data over the neonatal period. *Neuroimage,* 186**,** 321-337.
Putnam, S. P. & Rothbart, M. K. 2006. Development of short and very short forms of the Children's Behavior Questionnaire. *J Pers Assess,* 87**,** 102-12.
Schuh, A., Makropoulos, A., Wright, R., Robinson, E. C., Tusor, N., Steinweg, J., et al. A deformable model for the reconstruction of the neonatal cortex. 2017 IEEE 14th International Symposium on Biomedical Imaging (ISBI 2017), 18-21 April 2017 2017. 800-803.
Seidlitz, J., Vasa, F., Shinn, M., Romero-Garcia, R., Whitaker, K. J., Vertes, P. E., et al. 2018. Morphometric Similarity Networks Detect Microscale Cortical Organization and Predict Inter-Individual Cognitive Variation. *Neuron,* 97**,** 231-247 e7.
Tournier, J. D., Christiaens, D., Hutter, J., Price, A. N., Cordero-Grande, L., Hughes, E., et al. 2020. A data-driven approach to optimising the encoding for multi-shell diffusion MRI with application to neonatal imaging. *NMR Biomed,* 33**,** e4348.
Van Essen, D. C., Smith, S. M., Barch, D. M., Behrens, T. E., Yacoub, E., Ugurbil, K., et al. 2013. The WU-Minn Human Connectome Project: an overview. *Neuroimage,* 80**,** 62-79.
Wang, Q., Xu, Y., Zhao, T., Xu, Z., He, Y. & Liao, X. 2021. Individual Uniqueness in the Neonatal Functional Connectome. *Cereb Cortex,* 31**,** 3701-3712.
Wass, S., Porayska-Pomsta, K. & Johnson, M. H. 2011. Training attentional control in infancy. *Curr Biol,* 21**,** 1543-7.
Williams, L. A., Gelman, N., Picot, P. A., Lee, D. S., Ewing, J. R., Han, V. K., et al. 2005. Neonatal brain: regional variability of in vivo MR imaging relaxation rates at 3.0 T--initial experience. *Radiology,* 235**,** 595-603.
Wolke, D., Jaekel, J., Hall, J. & Baumann, N. 2013. Effects of sensitive parenting on the academic resilience of very preterm and very low birth weight adolescents. *J Adolesc Health,* 53**,** 642-7.
Zhu, K., Dougherty, R. F., Wu, H., Middione, M. J., Takahashi, A. M., Zhang, T., et al. 2016. Hybrid-Space SENSE Reconstruction for Simultaneous Multi-Slice MRI. *IEEE Trans Med Imaging,* 35**,** 1824-36.

Figure 1.TIF

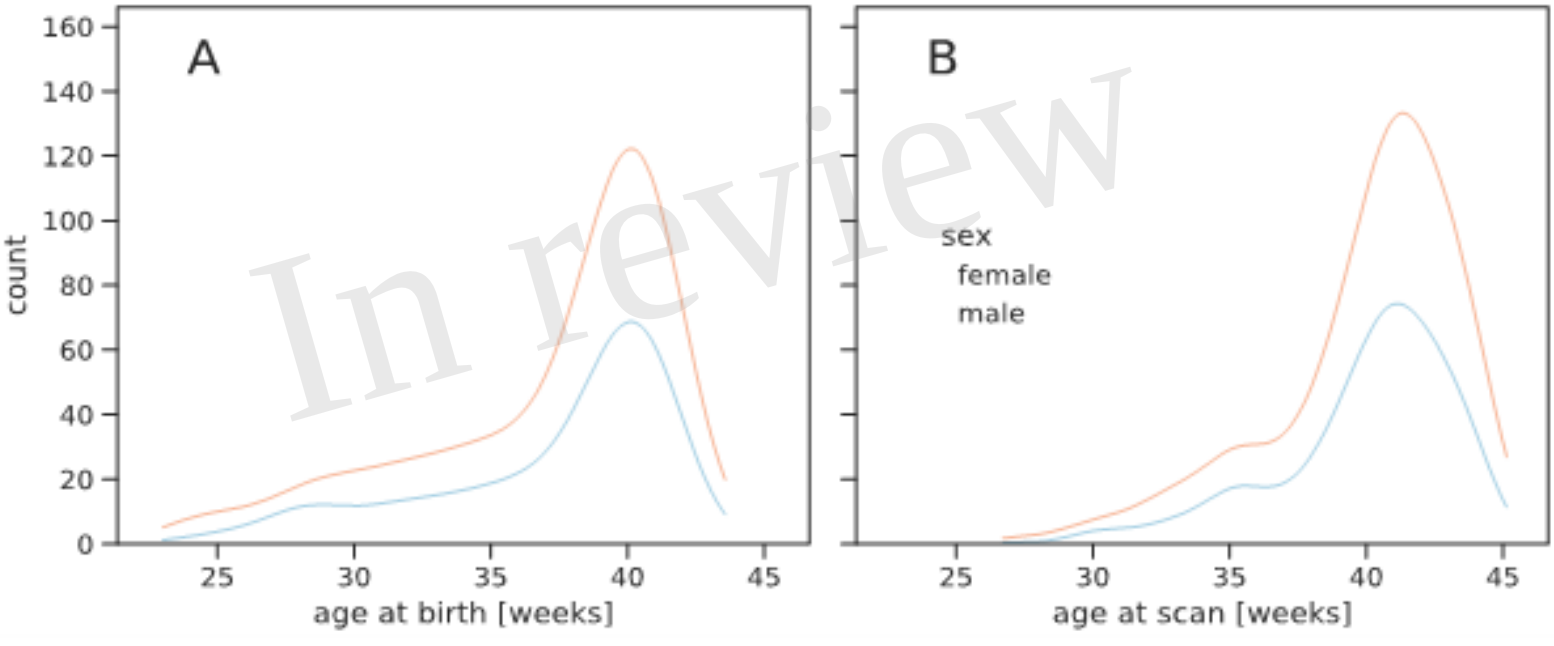

Figure 2.TIF

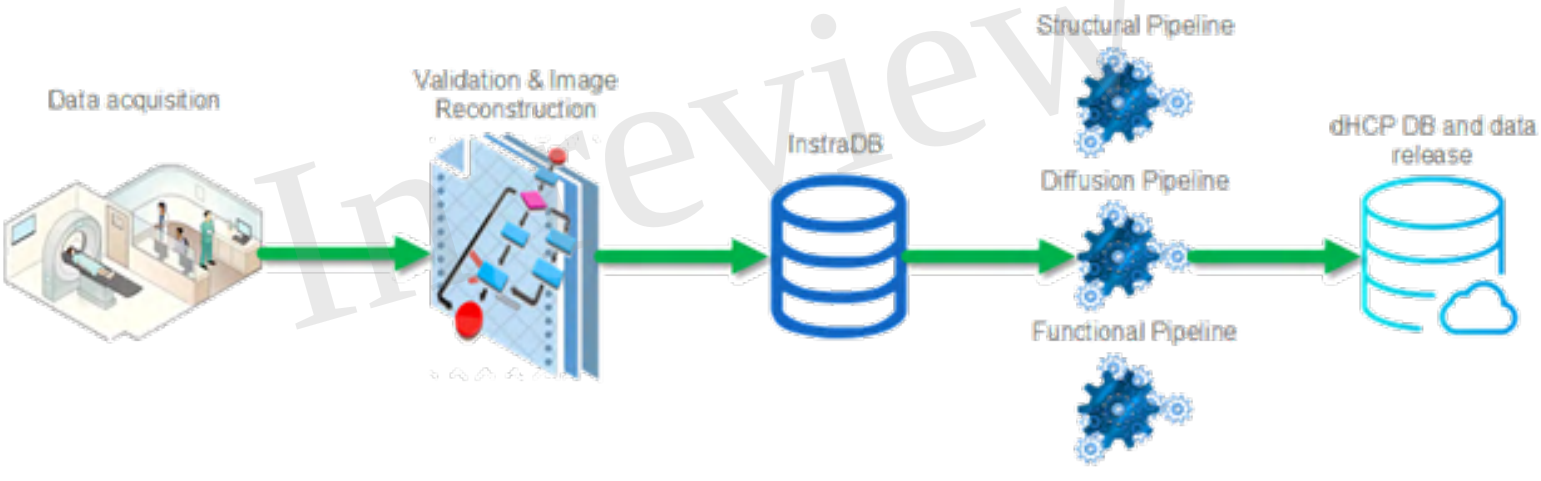

Figure 3.TIF

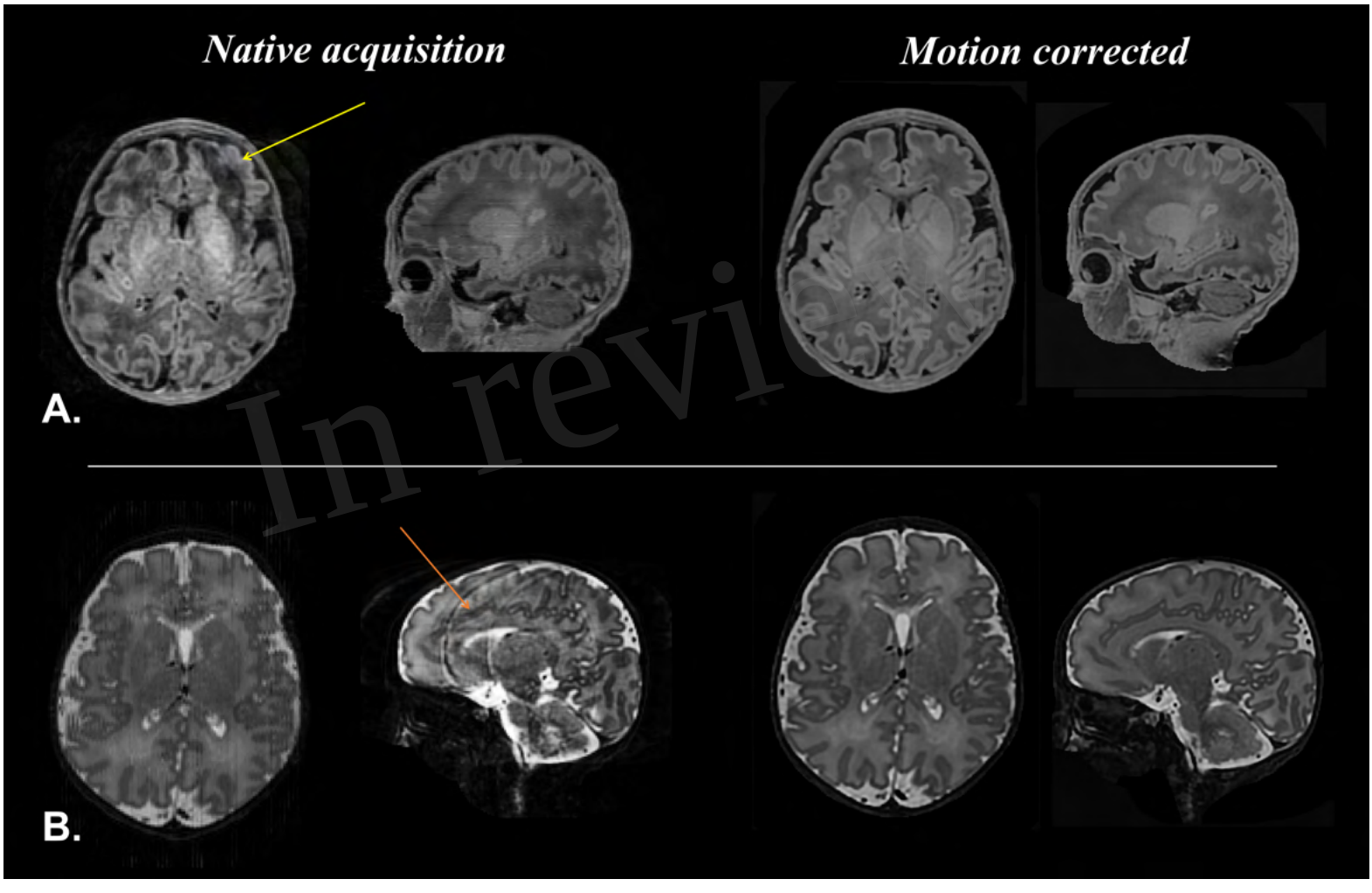

Figure 4.TIF

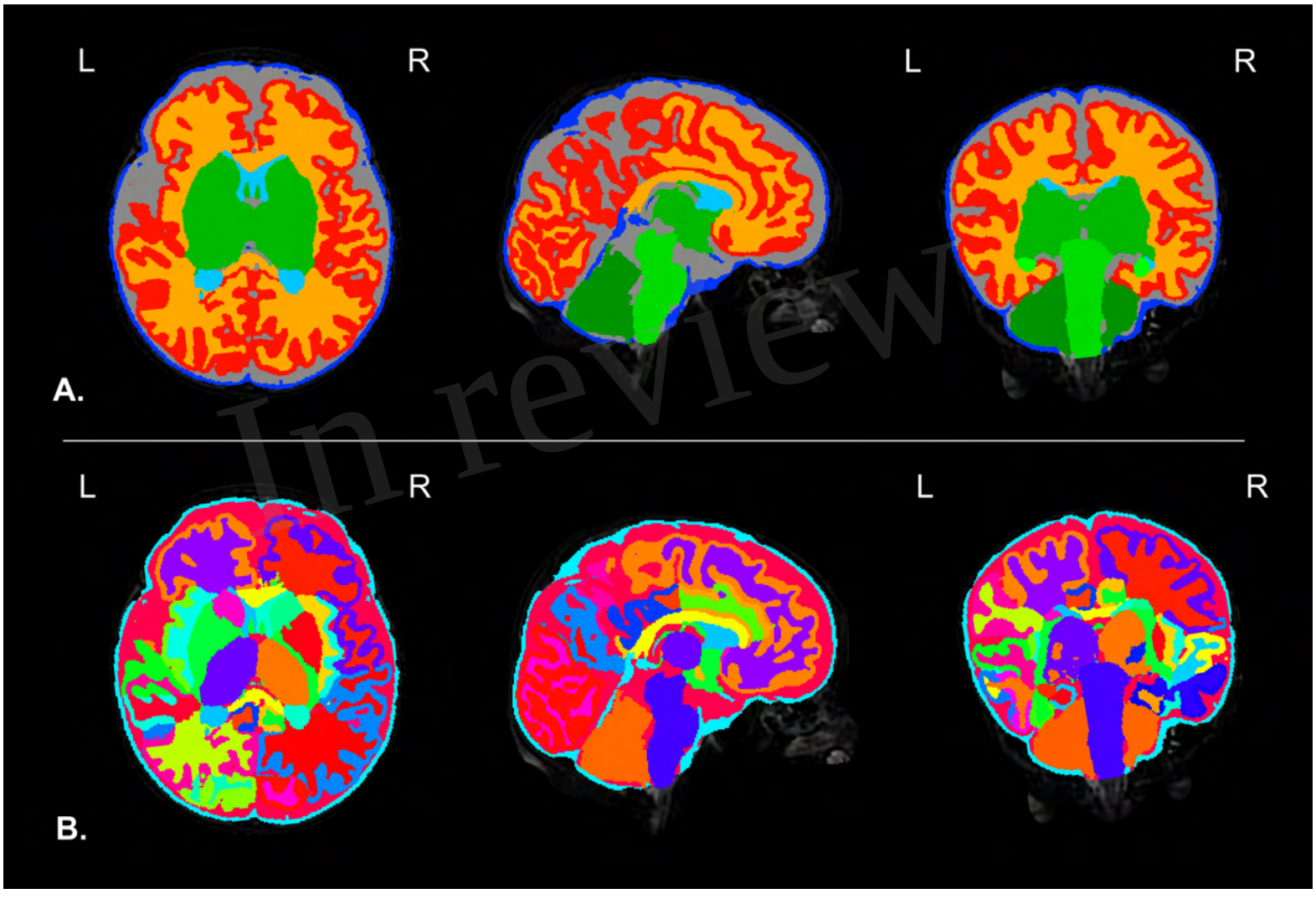

Figure 5.TIF

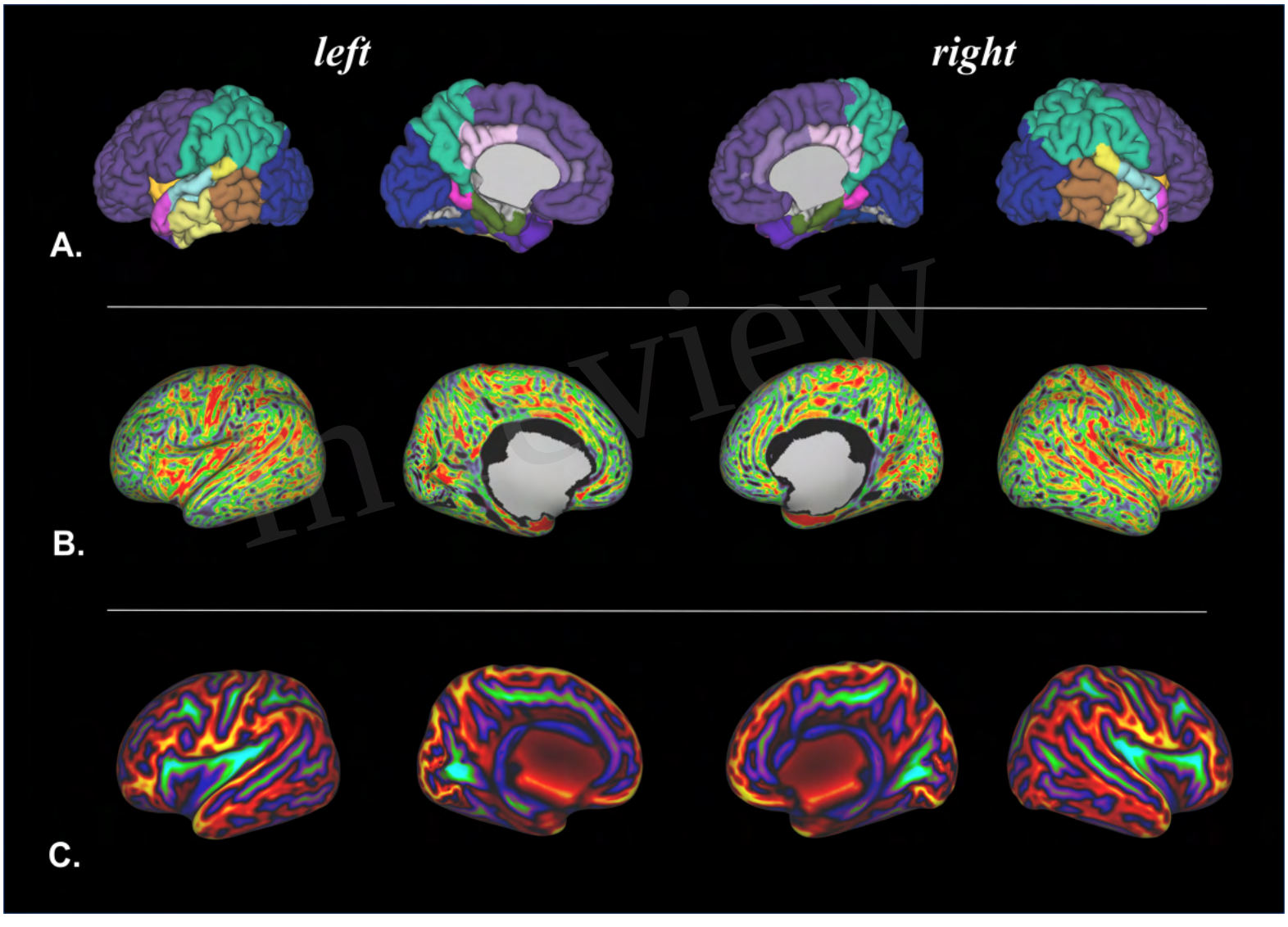

Figure 6.TIF

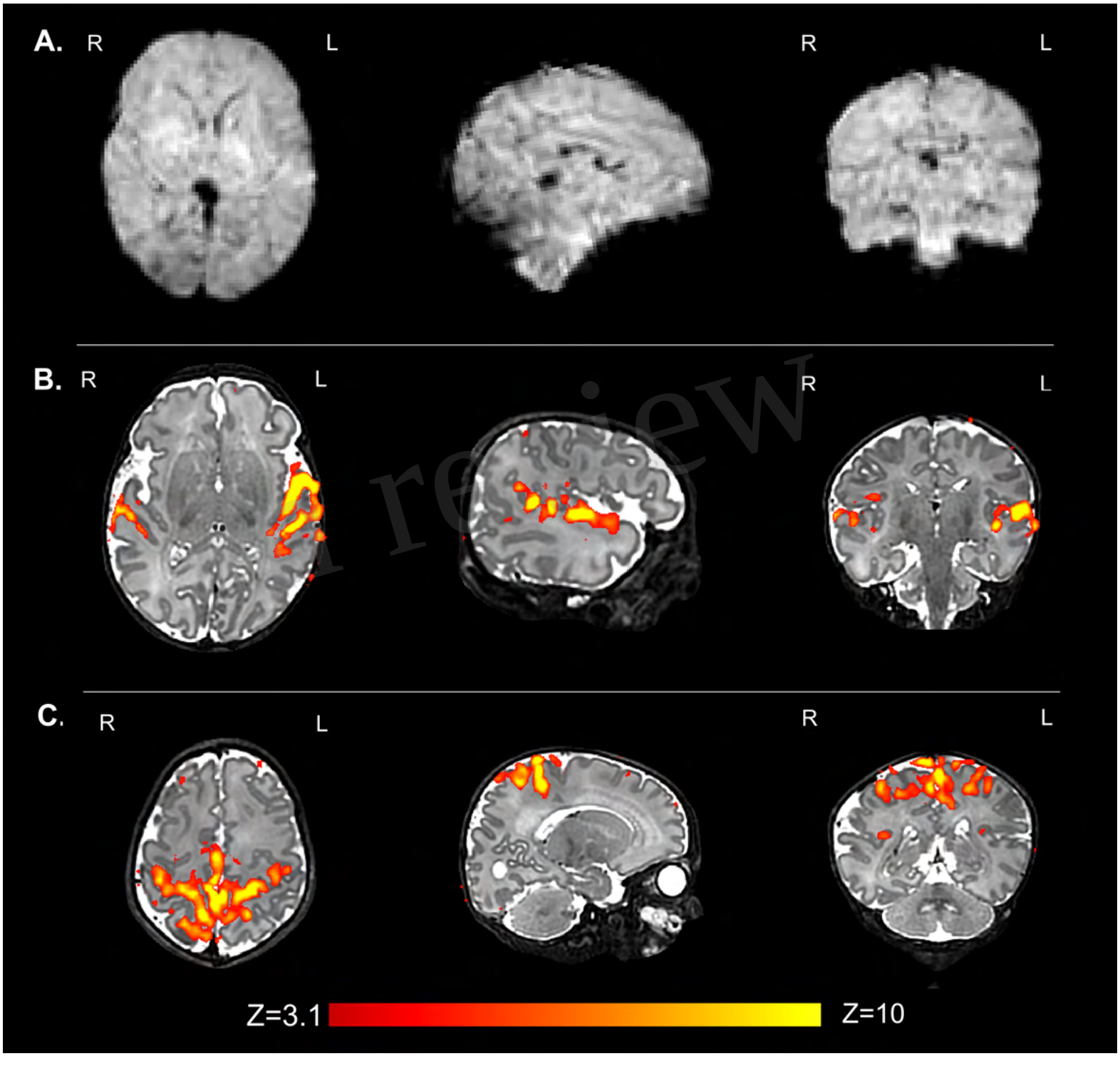

Figure 7.TIF

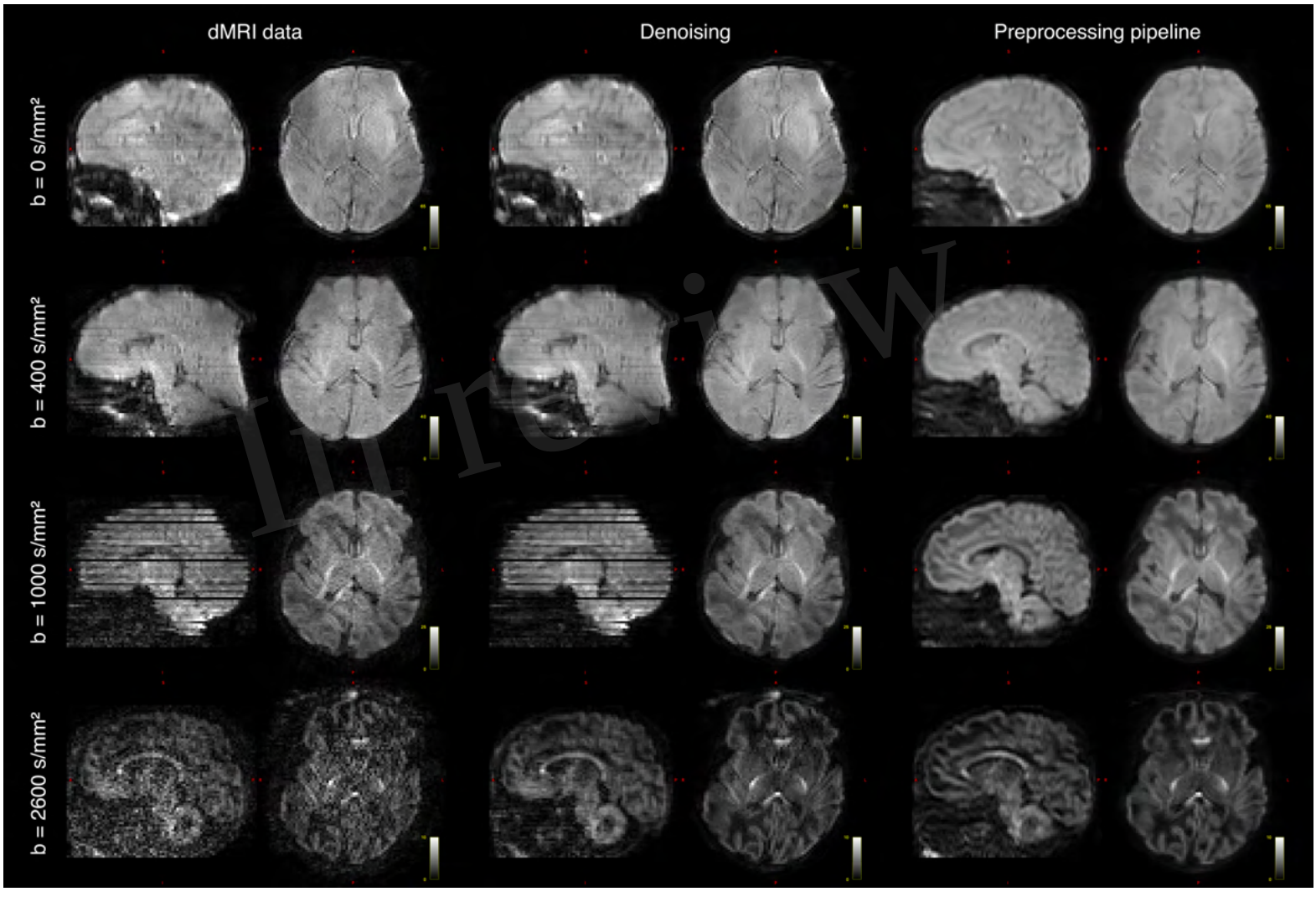
dMRI data
Denoising
Preprocessing pipeline
b = 0 s/mm²
b = 400 s/mm²
b = 1000 s/mm²
b = 2600 s/mm²

Figure 8.TIF

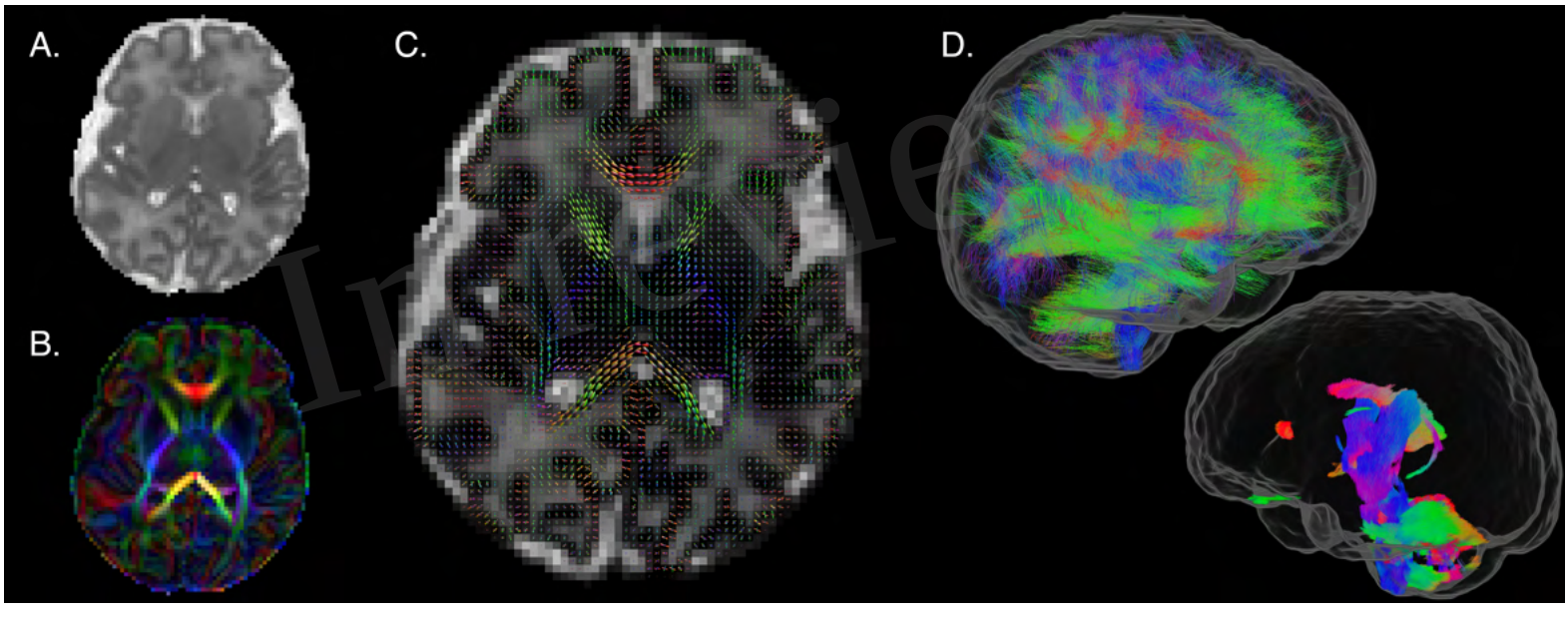

Figure 9.TIF

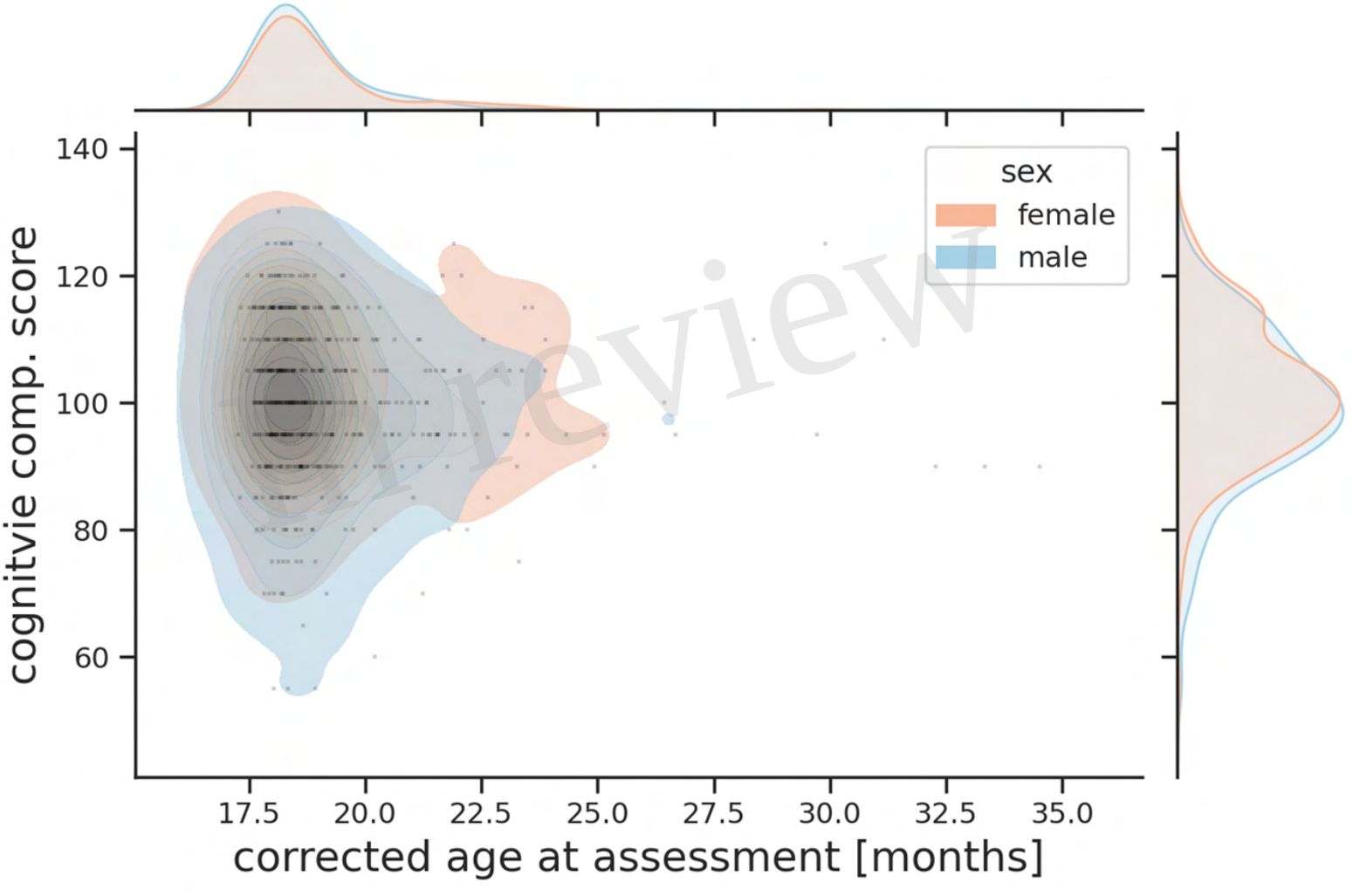

Figure 10.TIF